12-2010

Analyzing the impact of reactive transport on the repository performance of TRISO fuel

Gregory Schmidt
University of Nevada, Las Vegas

ANALYZING THE IMPACT OF REACTIVE TRANSPORT ON THE REPOSITORY PERFORMANCE OF TRISO FUEL

.

by

Gregory Schmidt

Bachelor of Science
Cornell University
2008

A thesis submitted in partial fulfillment of
the requirements for the

Master of Science in Materials and Nuclear Engineering
Department of Mechanical Engineering
Howard R. Hughes College of Engineering

Graduate College
University of Nevada, Las Vegas
December 2010

UNLV
UNIVERSITY OF NEVADA LAS VEGAS

THE GRADUATE COLLEGE

We recommend the thesis prepared under our supervision by

Gregory Schmidt

entitled

Analyzing the Impact of Reactive Transport on the Repository Performance of TRISO Fuel

be accepted in partial fulfillment of the requirements for the degree of

Master of Science in Materials and Nuclear Engineering
Department of Mechanical Engineering

William Culbreth, Committee Chair

Ralf Sudowe, Committee Member

Yitung Chen, Committee Member

Robert Boehm, Committee Member

Gary Cerefice, Graduate Faculty Representative

Ronald Smith, Ph. D., Vice President for Research and Graduate Studies
and Dean of the Graduate College

December 2010

ABSTRACT

Analyzing the Impact of Reactive Transport on the Repository Performance of TRISO Fuel

by

Gregory Schmidt

Dr. William Culbreth, Examination Committee Chair
Professor of Mechanical Engineering
University of Nevada, Las Vegas

One of the largest determiners of the amount of electricity generated by current nuclear reactors is the efficiency of the thermodynamic cycle used for power generation. Current light water reactors (LWR) have an efficiency of 35% or less for the conversion of heat energy generated by the reactor to electrical energy. If this efficiency could be improved, more power could be generated from equivalent volumes of nuclear fuel. One method of improving this efficiency is to use a coolant flow that operates at a much higher temperature for electricity production. A reactor design that is currently proposed to take advantage of this efficiency is a graphite-moderated, helium-cooled reactor known as a High Temperature Gas Reactor (HTGR). There are significant differences between current LWR's and the proposed HTGR's but most especially in the composition of the nuclear fuel. For LWR's, the fuel elements consist of pellets of uranium dioxide or plutonium dioxide that are placed in long tubes made of zirconium metal alloys . For HTGR's, the fuel, known as TRISO (TRIstructural-ISOtropic) fuel, consists of an inner sphere of fissile material, a layer of dense pyrolytic carbon (PyC), a ceramic layer of silicon carbide (SiC) and a final dense outer

layer of PyC. These TRISO particles are then compacted with graphite into fuel rods that are then placed in channels in graphite blocks. The blocks are then arranged in an annular fashion to form a reactor core.

However, this new fuel form has unanswered questions on the environmental post-burn-up behavior. The key question for current once-through fuel operations is how these large irradiated graphite blocks with spent fuel inside will behave in a repository environment. Data in the literature to answer this question is lacking, but nevertheless this is an important question that must be answered before wide-spread adoption of HTGR's could be considered.

This research has focused on answering the question of how the large quantity of graphite surrounding the spent HTGR fuel will impact the release of aqueous uranium from the TRISO fuel. In order to answer this question, the sorption and partitioning behavior of uranium to graphite under a variety of conditions was investigated. Key systematic variables that were analyzed include solution pH, dissolved carbonate concentration, uranium metal concentration and ionic strength. The kinetics and desorption characteristics of uranium/graphite partitioning were studied as well. The graphite used in these experiments was also characterized by a variety of techniques and conclusions are drawn about the relevant surface chemistry of graphite. This data was then used to generate a model for the reactive transport of uranium in a graphite matrix. This model was implemented with the software code CXTFIT and validated through the use of column studies mirroring the predicted system.

ACKNOWLEDGEMENTS

I would like to express my deepest thanks and gratitude to my advisor, Dr. Gary Cerefice for both offering me the opportunity to do this research and his constant assistance throughout the process.

To my parents, Ken and Diane, for all their love and support

To my brother, Scott, for encouraging me to come to Las Vegas when the opportunity presented itself

To all my friends, for the many good times along the way

TABLE OF CONTENTS

LIST OF TABLES

LIST OF FIGURES

VARIABLE DICTIONARY

α	Dispersivity, cm
θ	Porosity of graphite when fully saturated, ml/ml
θ_f	Volumetric water content, L^3/L^3
v	Pore-water velocity, L/T
ρ	Dry bulk density of graphite in column, g/ml, M/L^3
σ	Surface charge
σ_d	Charge density of counter-ions
σ_H	Surface charge from adsorbed hydrogen ions
σ_{is}	Surface charge contributed from inner-sphere complexes
σ_{os}	Surface charge from outer-sphere cation-anion complexation
Ψ	Electrical surface potential
Ψ_d	Surface complex potential at counter ion layer
Ψ_0	Surface complex potential at sorbing surface
Ψ_{os}	Surface complex potential at outer sphere layer
b	Empirical langmuir parameter, µg/g
C_1	Integral capacitance of inner-sphere layer
C_2	Integral capacitance of outer-sphere layer
C_{in}	Initial concentration of uranium in solution, µg/ml
C_{fi}	Concentration of uranium in solution after equilibration, µg/ml
c_r	Resident concentration M/L^3
D	Mechanical dispersion coefficient, cm^2/hr, L^2/T
F	Faraday constant, 96,485 C/mol
I	Ionic strength of solution
J_w	Solution flux, $M/ L^2 T$
K_d	Partition coefficient, ml/g
K_F	Empirical Freundlich parameter, ml/g
K_L	Empirical Langmuir parameter, ml/g
M	Mass, M
M_g	Mass of graphite, g
N	Empirical Freundlich parameter, dimensionless
q	Mass uranium sorbed per mass graphite, µg/g
R	Retardation factor, dimensionless
R	Ideal gas constant, 8.314 J/ mol
s	Concentration sorbed phase, M/M
T	Temperature, K
t	Time, T
V_{sol}	Volume of Uranium Solution in Batch Experiment, ml
X	Distance, L
z	Charge of solution electrolyte

CHAPTER 1

INTRODUCTION

1.1 Problem Statement and Research Objectives

With the growing interest in the further development of nuclear power both within the United States and throughout the world, there has been an increased focus on new and improved reactor designs. One of the designs currently proposed as a Generation IV nuclear reactor is a graphite-moderated and helium-cooled design known as a High-Temperature Reactor (HTR). The basics of this design were first proposed by Oak Ridge National Laboratory in 1947 and since that time several HTR's have been built and operated (Morris and Bauer, 2005). The main utility of these reactors and why they continue to generate significant interest is their increased efficiency in power generation over current light-water reactors (LWR). Independent studies of efficiency by Oak Ridge National Laboratory, the Massachusetts Institute of Technology and General Atomics have indicated that a high efficiency of 47.7% is achievable for power generation (General Atomics, 1996). When contrasted with the approximately 32% efficiency currently achieved in light water reactors, this fact makes a compelling argument for the adoption of HTR (Bodansky, 2004).

While HTR do have many theoretical marks in their favor, there are several areas of basic research that need to be completed before wide-spread adoption could be contemplated. In particular, the HTR fuel elements are so different from standard spent nuclear fuel (SNF) that significant research remains to be done on the repository performance of HTR fuel. HTR fuel is composed of

microspheres of fuel material surrounded by a porous carbon buffer to permit space for fission products and gases followed by a layer of SiC squeezed between two layers of pyrolytic carbon (PyC). These particles are known as TRISO particles (TRIstructural-ISOtropic). These particles are then embedded in a graphite compact which is itself inserted into a fuel channel drilled into a much larger graphite fuel element. These elements are then arranged in an annular fashion to form a reactor core (General Atomics, 1996). Dimensions of these system components are included in Table 1.1 and images are included in Figure 1.1.

Fuel Particles	
Kernel Radius, μm	175
Buffer Thickness, μm	100
Inner Pyrocarbon Coating Thickness, μm	35
SiC Coating Thickness, μm	35
Outer Pyrocarbon Coating Thickness, μm	40
Fuel Compacts	
Diameter, mm	12.45
Height, mm	49.3
Hexagonal Fuel Assembly Blocks (Elements)	
Flat to Flat, mm	360
Height, mm	790
Graphite Thickness Between Fuel and Coolant Channels, mm	4.5

Table 1.1: Dimensions for TRISO particles and fuel elements (Morris and Bauer, 2005)

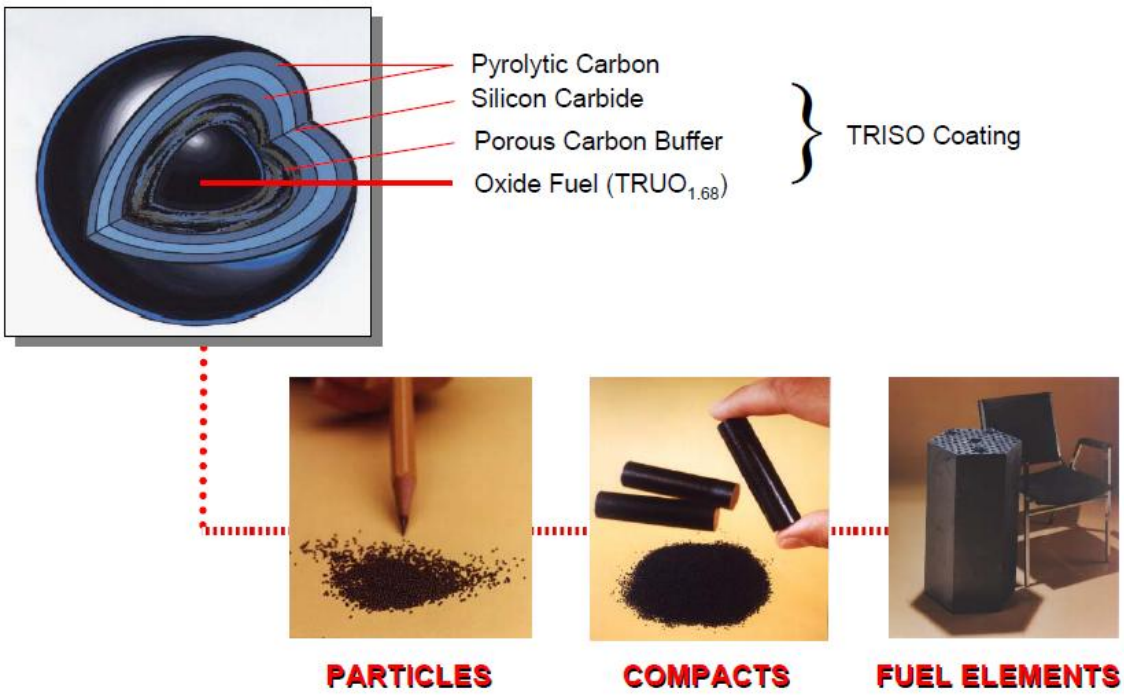

Figure 1.1: Images of TRISO particles, compacts and assemblies (Morris and Bauer, 2005)

These extreme differences between SNF and TRISO fuel render current models for the release of radionuclides from SNF inappropriate to the calculation of radionuclide release from TRISO fuels.

While some modeling research suggests that the radionuclide release from TRISO fuel could be several orders of magnitude better than SNF (Morris and Bauer, 2005), basic questions remain to be answered before a quantitative understanding of the rate and amount of release of radionuclides from TRISO fuel can be accomplished. Accordingly, this research has the following goals:

- Evaluation through batch experiments of uranium sorption and distribution coefficients (K_d) to graphite
- Determination of the rate and kinetics of uranium sorption to graphite

- Determination of uranium desorption rates from graphite using batch experiments to measure rates and column experiments to measure the distribution of rates
- Determination of the significance of uranium transport retardation through a graphite matrix by column studies
- Deriving a mass balance for the desorption of uranium from graphite to evaluate the possibilities of longer-term more irreversible sorption between uranium and graphite
- Evaluate the key parameters governing rates and magnitude of uranium sorption and desorption to graphite
- Evaluating the effects of diffusion and water velocity in the matrix on uranium release and sorption
- Creating a valid model that incorporates the knowledge gained through experimental work and then validating it using the program CXTFIT

1.2 Background and Theory

1.2.1 Theory of Sorption

Sorption is a term that includes several different mechanisms, such as electrostatic attraction, surface complexation and precipitation, for the removal of an aqueous ion from solution by a reacting surface (Essington, 2003). In discussion of heavy metals such as uranium, electrostatic adsorption and surface complexation generally refer to the formation of so-called “outer-sphere” and “inner-sphere” complexes respectively in solution. The sphere that is referenced in this nomenclature is the six waters of hydration that generally surround any ion

in solution in an octahedral shape. These waters are usually strongly coordinated by the ion in solution however; the ion in solution does have an influence that can extend out beyond the primary coordination sphere represented by the waters. This attraction beyond the inner hydration sphere is electrostatic in nature and in a pure solution can lead to rough polarization of the local water molecules or in the case of sorption, an electrostatic attraction to a surface. As this attraction does not involve primary coordination of the ion in solution, it is referred to as outer-sphere and is generally of a weaker nature than inner-sphere complexation (Essington, 2003 and Langmuir, 1997). Due to the stronger coordination between the water molecules in the inner hydration sphere and the aqueous ion, the replacement of one of those water molecules by a sorbing surface yields a much stronger interaction than outer-sphere complexation. It should be noted that these sorptive mechanisms are not exclusive and can occur simultaneously between a reactive surface and ions in solution.

There are several models used to quantitatively describe sorption by surface complexation and electrostatic adsorption in solution by a surface including Constant Capacitance (CC) Models, Diffuse Layer (DL) Models and Triple Layer (TL) Models. These models and their characteristics and requirements will be summarized in Section 1.2.4.

Due to previous uranium studies, it is not expected that sorption could be well-described by a precipitation model and accordingly investigative efforts will focus on surface complexation reactions and electrostatic interactions as the dominant solution reactions.

1.2.2 Previous Uranium Sorption Studies and Reactive Transport

Uranium is a radionuclide of great importance due to its position as the bulk of the heavy metal in spent fuel and its toxicity. For these reasons, many studies of uranium sorption have been completed on different geological media. Materials such as alpha-alumina, sediments from mill tailings, soil, granite, hematite and magnetite have all been investigated due to their geologic importance and prominence (Ackay, 1998, Baik *et al.*, 2003, Hyun *et al.*, 2009). While these studies are informative in their detailing of several important parameters for uranium sorption and their experimental methodology, the variety and complexity of the systems used makes extrapolation from that work to uranium behavior with graphite inappropriate. For instance, there has been strong research into the effect of microbial activity and normal organic matter on the sorption of uranium in geological media (Francis, 1999, Murphy *et al.*, 1998). Due to the extreme radioactivity of spent TRISO fuel and its isolation before emplacement in a repository environment, neither of these factors is believed to play a significant role in uranium sorption under repository conditions. However, their potential influences on other studies of uranium transport cannot be ignored. For this reason, the literature apparently lacking in any study of uranium sorption/desorption to graphite, experimentally generated numbers are a necessity.

Batch experiments are one of the most common methods of measuring sorption to different media and in this case, it is believed will also provide a valid method of measuring uranium sorption to graphite. Measurements will be taken

of uranium sorbed per mass graphite and distribution coefficient (K_d) values through a basic experimental model of allowing known quantities of uranium in solution to equilibrate with graphite of a known surface area and mass and then measuring the change in solution concentration. Equation 1.1 expresses the relationship between the initial concentrations, final concentrations, volume of solution, graphite mass and uranium mass sorbed to the graphite.

$$q = \frac{(C_{in} - C_{fi})V_{sol}}{M_g} \qquad Equation\ 1.1$$

Where,
q = Mass uranium sorbed per mass graphite, µg/g
C_{in} = Initial conc. of uranium solution, µg/ml
C_{fi} = Conc. of solution after equilibration, µg/ml
V_{sol} = Volume of uranium solution in batch experiment, ml
M_g = Mass of graphite, g

For this thesis, sorption for a range of uranium concentrations ranging from 500 ppb to 50 ppm U in solution will be measured under various aqueous conditions. The advantage of employing these ranges is that it is possible to develop an understanding of the adsorption isotherm, which is a graphical or mathematical way of expressing the amount of sorbate on a sorbing surface at a constant temperature or pressure, for given sorbate/surface interactions. In this case, the two most common types of curves for sorption are the L-curve and S-curve isotherms (Essington, 2003), which are shown as Figure 1.2.

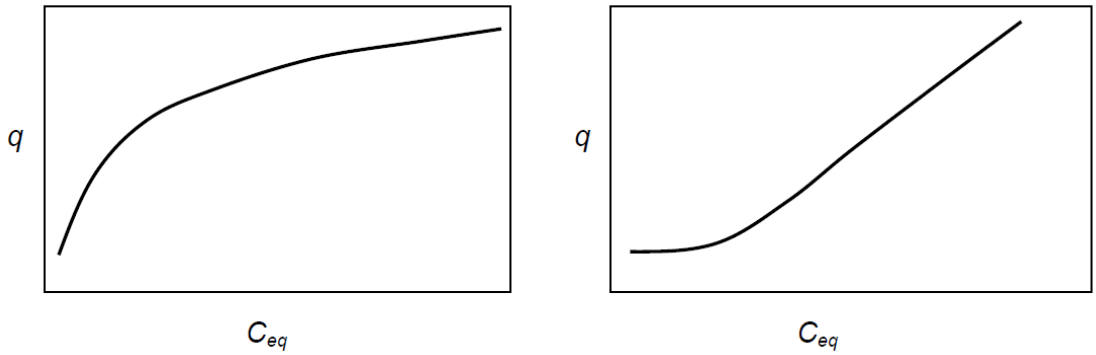

Figure 1.2: L-curve and S-curve isotherms respectively

Each of which would imply different facts about the mechanism of uranium sorption to graphite. If an L-curve is found, this indicates that the sorbate has a higher affinity for the sorbing surface when surface coverage is incomplete. An S-curve would be indicative of the opposite i.e. Low affinity between sorbate and surface at low surface coverage (Essington, 2003). An S-type isotherm is most commonly found for trace elements in the environment where complexing competition between other dissolved species can be found. The competitive species limit sorption until the concentration of the element of interest in solution becomes sufficient to satisfy all competing complexation demands. For a homogenous experimental set-up like the one proposed in this case, this type of isotherm would be of interest due the limited number of possibilities for other elements to complex the uranium in solution. It could potentially be indicative of carbonate interference at certain pH values. However, this is not the only possibility as ionic interferences can also cause this type of isotherm but it would provide further avenues of investigation (Essington, 2003). It should be noted

that while the proposed concentrations of uranium in solution are far above what could be reasonably expected from the groundwater in even the most contaminated of sites, they are eminently reasonable concentrations for water moving through a TRISO fuel compact with its large load of uranium.

Once the values for q are established, this data can then be used to calculate the bulk distribution coefficient. The bulk distribution coefficient is measure of material sorbed to the soil compared to material still in solution and can be calculated by Equation 1.2.

$$K_d = \frac{\left(\frac{(C_{in} - C_{fi})V_{sol}}{M_g}\right)}{C_{fi}} \qquad Equation\ 1.2$$

Where, terms are described above in Equation 1.1
K_d = Distribution coefficient, ml/g

The study of uranium desorption is unfortunately not as thorough as the study of sorption but the existing literature does have several examples of desorption experiments with uranium. Many of the studies involved use material loaded with uranium in previous sorption experiments and then the uranium solution is exchanged for a blank solution which has its solution concentration of uranium measured over time to quantify uranium desorption. This provides a quantitative way of measuring the release from materials loaded with known amounts of material over known surface areas. Unfortunately, as described above, mechanisms of sorption and desorption are difficult to determine with certainty due to the many variables affecting the interactions and the fact there are potentially many different mechanisms of reaction occurring simultaneously.

So while there might be many different mechanisms of interaction all occurring at a different rate, the bulk behavior is simply grouped into one effective K_d value that might be composed of many other K_d values acting in concert. For instance, one simplification that is commonly used is reducing the interactions to a combination of sorption through a fast acting sorption/desorption process combined with a slower more irreversible sorption. While in this case, the fast acting kinetics would govern the speed of transport the slower more permanent sorption would have a great effect on restricting the mass of metal being transported which is obviously of great importance for the modeling of contaminants in the environment. For this reason, the data gathered from batch sorption/desorption experiments will then be compared with kinetics and column experiments to validate the data gathered and to determine the retardation factor associated with uranium transport through graphite. The retardation factor is the ratio of distance traveled by a non-reactive substance (usually water) to a reactive substance (uranium, in this case). Equation 1.3 expresses the relationship between distribution coefficient, graphite bulk density, porosity and retardation.

$$R = 1 + \left(\frac{\rho}{\theta}\right) K_d \qquad Equation\ 1.3$$

Where,
R = Retardation factor
ρ = dry bulk density of graphite in column
θ = porosity of graphite when fully saturated
K_d = distribution coefficient

This equation has also been expressed in a conservative manner as follows in Equation 1.4 (Bodansky, 2004)

$$R = 1 + 10K_d \qquad Equation\ 1.4$$

This simplification results from the empirical observation that values of ρ are usually greater than 2 g/ml and the value of θ is usually less than 0.2. To generalize results obtained from batch experiments, this conservative equation will be used to produce estimated retardation factors for uranium moving through graphite.

By examining the differences between calculated retardation using the K_d from the batch experiments and the measured retardation from column experiments, deviations from the single ideal K_d value will be assessed. This information will be combined with kinetics and desorption data to produce a transport model.

1.2.3 Environmental Effects on Uranium Speciation and Sorption

Previous research has indicated that the systematic parameters of greatest interest for uranium sorption and speciation are uranium concentration, carbonate concentration, pH and surface area of the adsorbing surface (Prikryl *et al.*, 1994). Other research has found that sorption is most prominent at or near neutral pH (pH = 5.5-8.8) with an expectation that different pH effects are limiting at low and high pH (Echevarria *et al.*, 2001). For low pH systems, where the UO_2^{2+} species dominates, sorption is inhibited; whereas for higher pH systems, the formation of carbonate complexes inhibits sorption (Prikryl *et al.*, 1994).

These conclusions are in broad agreement with other studies of uranium sorption (Baik *et al*., 2003 and Waite *et al*., 1994). They also indicate the degree to which pH influences the sorption behavior of uranium. As can be seen in the speciation curve for uranium under the experimental conditions included as Figure 1.3, generated using the EQ3/6 geochemical modeling software (Wolery & Daveler, 1992) with the database developed for the Yucca Mountain Project, uranium forms many species in solution and small changes in pH can lead to large changes in the relative concentrations of uranium species in solution.

For this reason, a range of pH values will be investigated ranging from 2.0-9.5. Points will also be selected to ensure the lack of pH effects on the graphite itself. Experiments will be carried out under both highly acidic and highly alkaline conditions where the expected speciation of uranium is the same because if sorption behavior is only a function of uranium speciation and there are no changes in graphite composition then the sorption characteristics should be uniform across pH ranges that consist of identical uranium species.

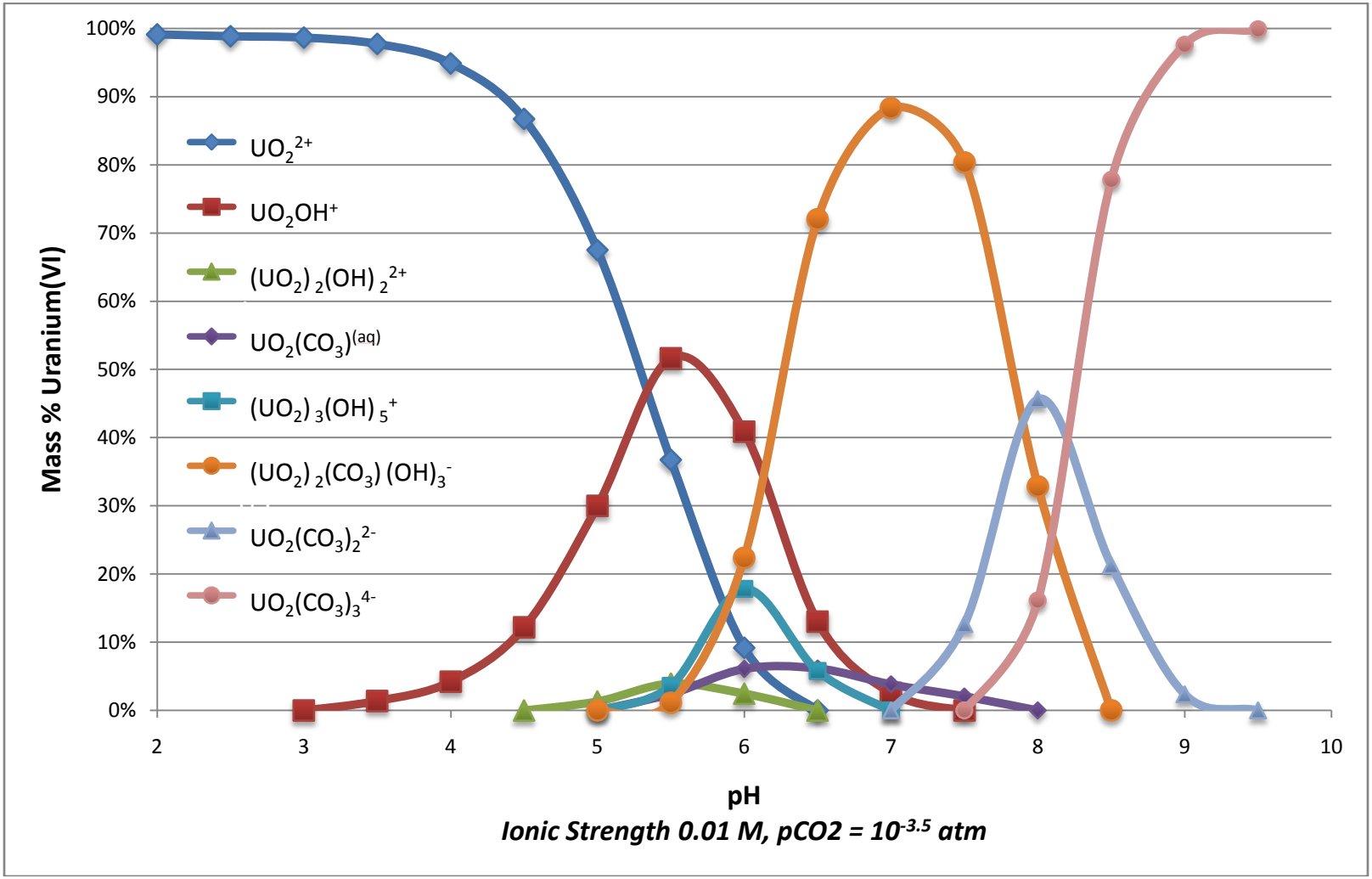

Figure 1.3: Uranium speciation under experimental batch sorption conditions [U] = 500 ppm

The surface area of the sorbing surface has also been identified as a key factor in the quantity of sorption occurring. Prikryl *et al.* (1994), noted that sorption increases as surface area to volume ratios are increased. In this case, surface areas for graphite from fuel elements have been observed to have a BET (BET details described in Section 2.3) surface area of 2.1-5.5 m^2 / g of BET surface area (Fachinger, *et al.* 2003). For this reason, high purity graphite with a well characterized BET surface area will be used in solution. The ratio of graphite surface area to uranium solution mass will also be held as constant as possible over the experimental process.

1.2.4 Summary and Analysis of Quantitative Adsorption Models

The first model mentioned above was the CC model. This model makes the assumption that all complexation amongst adsorbed species is of an inner-sphere nature with outer-sphere complexes being ignored. Surface charge is created by the specific adsorption of protons and solution ions with the surface charge density being related to the potential at the surface. An intrinsic equilibrium constant for the complexation reaction is identified and can be thought of as a stability constant for the surface-ion complex that is formed.

The second model mentioned is the DL model. This model accounts for solution sorption by the formation of a strong inner-sphere complex with constant surface potential to a specific radius with the complexation of counter-ions and other aqueous species occurring outside that radius due to electrostatic effects that fade at a distance. This model allows for consideration of inner-sphere complexation and outer-sphere complexation through electrostatic attraction.

The TL model is an elaboration of the DL model with, as its name suggests, a third layer of sorbing charge surrounding the surface. In contrast to the DL model which holds surface potential constant to a certain radius and then linearly decays away, the TL model includes two proximate regions of linear decay of surface charge followed by a region of exponential decay of surface charge. This allows for the consideration of differently bound inner-sphere complexes while also including outer-sphere complexed ions.

The above descriptions are simplistic and more detail can be found in Davis & Kent, 1990, Langmuir, 1997 and Essington, 2003. It should also be noted that the application details of each of these models can be changed and adapted to relevant conditions but many specific applications are highly dependent on ion-surface interactions and broad conclusions about the models can be difficult to make. However, the models do have some characteristics in common (Langmuir, 1997):

1) The sorbing surface is composed of functional groups that form immobile complexes in a similar manner to ion speciation in solution
2) These reactions can be described by bulk equations and modified by the inclusion of electrostatic effects
3) Surface charge and potential are the result of chemical surface reactions

A goal of this research is to determine the general and specific applicability of these surface complexation models to graphite-uranium solution interactions and,

if possible from the experimental data generated, implement an appropriate surface complexation model.

1.2.5 Previous Modeling Studies on TRISO Fuel

There have been few specific studies in the literature that attempt to completely model the failure and release of TRISO fuel. Because the microparticles are the location of the majority of TRISO fuel's inventory of material, more research has been dedicated to the microparticles themselves. Fachinger *et al.* (2006) investigated many of the individual components of a TRISO fuel system and their data provides valuable information on modeling the failure of the TRISO particle. It is recognized that the source term for release from a TRISO fuel form in a repository is governed by the failure rates of the coating after which the dissolution of the fuel kernel will be of the most importance. Of course, this leaching will only occur after the outer TRISO coatings have failed. The same study also examined the rates and mechanisms of failure of TRISO coatings. Information from this study on the dissolution of TRISO coatings and kernels under selected conditions is contained within Table 1.2 (more complete data can be found in the reference). This data on dissolution can be combined with particle lifetime to generate an expected lifetime for each TRISO particle.

Material	Solution	Atmosphere	Leaching rate
Pyrocarbon	DI Water	Oxygen	4.70×10^{-7} (g/ (m^2·day))
SiC	DI Water	Oxygen	5.05×10^{-6} (g/ (m^2·day))
Kernel	DI Water	Oxygen	1.40×10^{-6} (mol/ (m^2·day))

Table 1.2: Selected data on TRISO leaching in deionized water (Fachinger et al., 2006)

However, this gradual dissolution of the particle is not the only method of release. The other major method is induced failure from heat or radiation during burn-up or defects in the manufacturing process which would lead to immediate dissolution of the kernel upon emplacement and contact with groundwater. For very high quality fuel elements, failure fractions have been observed as 6×10^{-5} or better (Nickel *et al.*, 2002 and Petti *et al.*, 2003). This information on failure fractions combined with the leaching data cited above and dimensions of TRISO particles will provide an estimate of the changing source term for uranium release over time.

It should be noted at this point that the study cited above is a study of German TRISO particles which to this point have out-performed American fuel particles in release and manufacturing defects by a thousand fold (Petti *et al.*, 2003). However, the Germans have a longer history and more experience manufacturing TRISO fuels than the US and their success rate should be obtainable by US-manufactured TRISO fuel.

This discussion has so far only focused on the TRISO kernel itself and ignored the large quantity of graphite that it is embedded in. There has been as

yet no research found in the literature discussing the effects of this large quantity of graphite if the fuel element is directly disposed of in a repository environment. The difficulty of separating the TRISO kernels from the compact has been noted by several authors (Lifang *et al.*, 2009 and Fachinger *et al.*, 2008). If it is decided that these difficulties are too significant to support the separation of the TRISO kernels from the compact, it will be necessary to incorporate reactive transport through this graphite matrix into a repository performance model. It will be a primary goal of this thesis to develop a reactive transport model of uranium in a graphite matrix and then examine the conditions under which the incorporation of reactive transport could be of significance to repository performance.

The model for TRISO performance developed as part of this thesis will be validated by the reactive transport modeling software CXTFIT. The program is versatile and will allow for not only validation of any proposed model but adaptation of that model to different flow conditions and a sensitivity analysis of the relative importance of parameters controlling release.

1.3 Scope of Work

The primary objective of this study is to develop a quantitative understanding of how the large quantities of graphite in a directly deposited TRISO fuel compact would impact uranium release. To develop this model, experimental data on uranium sorption and transport through a graphite matrix will be developed along with an understanding of what systematic effects have the largest influence on uranium sorption and transport. Simulations will be run with the software CXTFIT (described in Section 2) to validate the model

generated and aid in understanding its implications for different environmental conditions. This will help provide information about when reactive transport between graphite and uranium should be included in the model of repository performance for TRISO fuel.

CHAPTER 2

MATERIALS AND METHODS

2.1 General Approach

To achieve the primary goal of this research as outlined above, it is necessary to have knowledge of how uranium in solution is partitioned between immobile (solid) phases and mobile (liquid) phases when exposed to graphite and the kinetics of that partitioning. As information in the literature is lacking on the subject of uranium/graphite chemical interactions, experimental studies were necessary to obtain this information. In addition, to be certain that it was indeed graphite/uranium interactions that were being examined the physical and electronic properties of the graphite used in these experiments was studied as well. Equilibrium uranium sorption and desorption to graphite was analyzed using batch experiments. The impact of water chemistry on uranium sorption to graphite was also examined during these batch experiments by changing solution conditions such as pH, dissolved CO_2 and ionic strength. Non-linearity in uranium partitioning to graphite was analyzed by changing the uranium metal concentration in solution and the kinetics of both the sorption and desorption reactions were studied by varying sample time. A model was developed from this data which was then applied to column studies incorporating reactive transport of uranium through a graphite matrix. Computer assisted methods, specifically the program CXTFIT, were used to validate and generalize the model that was developed from the experimental work.

2.2 Materials

Graphite

Initial experiments were conducted with the smallest particle diameter ground flake graphite available from Alfa Aesar. At this point it was noted that graphite has several characteristics which make aqueous experimentation difficult including an extreme hydrophobicity as well as a resistance to separation by centrifugation. Centrifugation was chosen as the desired separative technique to minimize the amount of contaminated radioactive waste generated during batch experiments. Next, coarser graphite was obtained from Alfa Aesar Lot #A12U026 with a mesh size -20+100 (0.853 mm > diameter > 0.152 mm) to permit more thorough mixing and facilitate separation by centrifugation. Experimental work also was done to confirm that centrifugation for 10 minutes at 4,000*G* achieved an indistinguishable separative effect from using a 0.45 μm syringe filter. This was the primary graphite used experimentally and unless otherwise indicated results refer to batch experiments performed with this graphite.

Water

All experiments were carried out with deionized water (DI) with a resistivity of 18 MΩ-cm that had been allowed to come to equilibrium with atmospheric CO_2 through either more than two hours of static equilibration in unsealed 1 L Nalgene containers or at least 15 minutes of active bubbling with an aquarium pump in an identical container. Solution ionic strength was controlled by the addition of sodium chloride (NaCl) to set ionic strength at 0.01 M for most

experiments. The effect of ionic strength on uranium partitioning was examined through a series of experiments that varied the ionic strength from 0.01 M through 4 M. The NaCl was obtained from Spectrum Lot #: RF1546. This was done to standardize any effects due to ionic strength on uranium speciation and sorption as those effects have been described in the literature as having an effect on uranium solution chemistry (Langmuir, 1997). This was necessary as otherwise small differences in ionic strength would have resulted from the use of variable amounts of HCl and NaOH in pH adjustment of contacting uranium solutions.

Radionuclides

For reasons that will be detailed in Section 2.5 under solution analysis, solutions with a uranium mass concentration fixed by a depleted uranium salt and activity fixed by addition of ^{233}U were used for batch experiments.

Uranium mass was controlled by use of a depleted uranium $UO_2(NO_3)_2$ salt that was prepared into an acidified (pH < 2) 1000 ppm working stock solution and diluted to reach desired uranium mass concentrations. Uranyl nitrate is known to be hygroscopic and before use the uranyl nitrate was baked at 50 °C for greater than 48 hours and was stored in a dessicator thereafter.

Uranium activity in solution was controlled by addition of spikes of a concentrated acidified ^{233}U solution prepared from a UO_2Cl_2 solid. Activity and ^{233}U concentration was verified by liquid scintillation counting (LSC) comparison to a known NIST traceable standard from Eckert & Ziegler. Ultima GOLD biodegradable organic scintillant from PerkinElmer with never less than a 10:1

scintillant to solution ratio was used as the scintillation cocktail for all LSC analysis.

Chemical Reagents

Sodium hydroxide (NaOH) and hydrochloric acid (HCl) were used for pH adjustment for all experiments.. Solutions of 0.01 M, 0.1 M and 1 M of each were prepared and used to adjust solution pH to the desired point and accounting for the dilution on the uranium mass.

Sodium tetraborate decahydrate (Borax) was used as a buffer for experiments with pH between 7 and 10 as dissociation of dissolved bicarbonate was resulting in changing pH over the experimental equilibration time.

2.3 Characterization of Graphite

Surface Area

Graphite surface area was characterized by using a multi-point adaptation of the the Brunauer-Emmett-Teller (BET, 1938) method of N_2 adsorption onto a surface using a Quantachrome NOVA 1100 high-speed gas sorption analyzer. Samples were thermally degassed at 300° C under a vacuum for greater than 48 hours to purge any initial adsorbed gas on the analyte surface. Multiple replicates of graphite were run with a calibrated silicon nitride standard (Specific Surface Area = 0.507 ± 0.085 m^2/g) from Quantachrome (Cat #: 2003 - Lot #: 2909) in order to determine the experimental error. Additionally, repeated measurements were taken of the same Quantachrome sample to measure machine precision.

Proton Exchange Capacity

Proton Exchange Capacity (PEC) of the graphite was measured by potentiometric titration in a well-mixed DI solution. A titration system from Metrohm USA consisting of a Titrino 799, a 685 Dosimat and an 801 Magnetic stirrer was used to dose 50 µl increments of 0.1 M NaOH and HCl into a graphite containing solution while measuring the change in pH. This was performed in a 0.01 M NaCl solution that had been purged with argon before titration. PEC was measured by comparing differences between theoretical changes in pH and measured changes in pH to quantitatively measure the number of hydrogen ions that are sorbed to the graphite surface (ie. The proton exchange capacity). Multiple replicates were used to estimate experimental uncertainty and titrations ranged across the entire pH of interest for these experiments (pH = 2-9).

Point of Zero Charge

The pH point of zero charge (PZC), the point at which below a surface has a net positive charge solution dependant charge and above has a negative solution dependant charge (Essington, 2003), was also measured using the same titration system as described above. As material surface charge is the product of both pH dependent and intrinsic surface factors, multiple potentiometric titrations of a material under different conditions of ionic strength will cross at the PZC due to variance in pH dependent surface charge with to ionic strength and no variance in the instrinsic surface charge (Essington, 2004). Titrations were done with 0.01 M NaOH and HCl solution into 0.01 M and 0.1 M

NaCl graphite containing solutions that had been well-purged with argon before titration.

Phase and Contaminant Analysis

A Bruker D8 Advance Powder X-Ray Diffraction (XRD) analyzer was used to characterize the experimental graphite used. XRD analysis consists of measuring the intensity of an X-ray beam that has diffracted off the sample. This intensity is then plotted as signal (in the form of counts) as a function of the incident X-ray angle. This diffraction pattern of X-ray strength vs. incident X-ray angle then shows information about the solid structure. Using Bruker's Topas software and EVA database, the diffraction data was analyzed to characterize the graphite and the potential existence of other contaminants.

Functionalization Analysis

Information from the literature suggests that graphite oxide and other compounds formed by the functionalization of graphite, which refers to the addition of chemical functional groups such as carboxyls, ether, alcohols, etc. to a surface, are strongly sorbing species that could potentially dominate the effects of graphite sorption. This functionalization increases the sorption behavior by providing additional surface sites for charge exchange which is the mechanism of both surface complexation and electrostatic adsorption as discussed in Section 1.2.1. Infrared spectroscopy using KBr pellet pressing was used to examine the graphite for any surface functional groups that might be the result of oxidation reactions on the graphite surface or otherwise have activated the graphite. This

information was compared to data available from the literature on the intrinsic IR spectra of graphite and graphite oxide.

2.4 Experimental Method

2.4.1 Batch Sorption

Batch sorption techniques were employed both to measure sorption kinetics and equilibrium partitioning of uranium and graphite but also to load graphite with uranium for use in multi-step desorption studies. Uranium tracer solutions of varied mass (50 ppb – 50 ppm) were loaded in an approximately 10:1 solution to solid mass ratio in polypropylene (PP) or fluorinated ethylene propylene (FEP) centrifuge tubes. 15 ml PP tubes were used for all experiments except when solution pH was between 6-8. At these pH's, 10 ml FEP containers were found to be necessary to reduce the strong sorption to the PP containers that occurred between those pH's. These loaded tubes were then placed onto hematology mixers and allowed to mix. Information on a period of time to permit sufficient equilibration was determined by repeated sampling of graphite contacting with uranium until changes in solution uranium concentration were undetectable. To study the time-dependence of sorption, both repeated sampling of batch containers and fast-flow column experiments were performed. Pictures of FEP tubes equilibrating on a hematology mixer are included on the following page as Figure 2.1. A picture of the PP centrifuge tubes used as well as sample Flex column of the type used in the column experiments described in 2.6 are shown as Figure 2.2.

Figure 2.1: Uranium contacting with graphite on a hematology mixer in FEP containers

Figure 2.2: PP Centrifuge Tube with Flex Column described in Section 2.6

Changing CO_2 Partial Pressure

As discussed in section 1.2.3, many authors have previously noted the apparent suppressive effect of uranyl carbonate species on uranium sorption (Waite *et al.*, 1994, Ackay, H. 1998, Prikryl & Pabalan 1999). This effect was investigated by changing relevant atmospheric concentrations of CO_2 using an MBRAUN glovebox and then performing batch experiments with water well-equilibrated to the local atmosphere. Experiments to measure sorption under an inert argon atmosphere with [CO_2] < 1 ppm were performed to confirm the inhibitory effect of dissolved carbonate and uranyl carbonate species on sorption. These experiments were performed in the alkaline region using a Borax buffer to keep pH constant. Additionally, experiments were performed under an atmosphere of >99.99% CO_2. These experiments were performed at neutral pH to attempt to suppress sorption and at acidic pH to aid in drawing conclusions about the sorbing species.

Changing Ionic Strength

The effects of ionic strength were examined by changing solution concentrations of NaCl before uranium equilibration with graphite occurred. Three experiments were performed with ionic strength equal to 0.01 molal, 0.05 molal and 0.1 molal for which no additional preparatory steps were required beyond increasing the amount of dissolved NaCl in solution. Two additional experiments were performed in 1 and 4 molal NaCl to examine the effects of a concentrated salt solution on sorption. As non-ideal effects in solution make the analysis of pH impossible using a standard non-equilibrated glass probe and pH

meter, a different method was necessary to ensure that pH was measured and adjusted properly. The Metrohm titration system described above for the PEC measurements was used to standardize the glass electrode used for pH measurement by the titration of known amounts of standardized base and acid in solutions of elevated ionic strength. These results were inputted into the GLass Electrode Evaluation (GLEE) program developed and distributed by Hyperquad. This allowed the calculation of theoretical Nernstian slope and intercept in the elevated salt conditions which are shown below in Table 2.1.

Salt Concentration (NaCl)	Nernstian Slope	Nernstian Intercept
1 molal	59.3 ± 0.4 mV / pH	- 442.8 ± 4 mV
4 molal	60.0 ± 0.4 mV / pH	- 461.9 ± 3 mV

Table 2.1: Nernstian slope calculations for elevated salt concentrations

After the electrode was calibrated, the conductance was directly read off the solution in mV and pH was solved for using the data given in the table above.

2.4.2 Multiple Step Batch Desorption

Graphite was allowed to come to contact with the uranium in solution for a period of time sufficient to permit equilibration. The samples were centrifuged to separate the graphite from the supernatant which was then decanted. Ionic strength controlled and pH tuned uranium-free solution was added to the graphite which was then shaken and allowed to re-equilibrate with the solution. Aliquots were taken after a period of time identical to the initial equilibration time and

uranium concentration in solution was measured. This procedure continued until the activity in solution was no longer measureable by LSC.

2.5 Solution/Concentration Analysis

Initial experiments to measure uranium concentration in solution used Inductively Coupled Plasma – Atomic Emission Spectroscopy (ICP-AES) techniques to measure initial and final uranium solution concentration directly. As the ICP-AES used was most sensitive to concentrations in the 25-200 ppm region, initial scoping experiments focused on this area. Results indicated that this concentration region was well above any equilibrium point for graphite/uranium sorption and that high experimental error due to the dilutions required for this technique was inhibiting proper analysis of the data and that a new technique was necessary. As the area of experimental interest appeared to lie in the 500 ppb to 50 ppm region, an analytical technique using a TriCarb LSC was devised. This required controlling uranium mass in solution by addition of concentrated DU spikes and activity by addition of concentrated ^{233}U spikes as described in the radionuclide section. Aliquots were taken after solutions were pH adjusted and prepared immediately before contacting with graphite and after a five-day equilibration time (unless otherwise indicated) with the solution in contact with graphite. Sorption to both the graphite and container was analyzed by measuring the change in solution activity via LSC. Samples were counted for at least 30 minutes or until a 2% error in experimental counts was achieved. Aliquots were sampled from each sample container and the final activity was

compared to the initial activity to determine the percentage of uranium in solution that sorbed for each experiment.

2.6 Column Studies

Initial column studies were performed in Synthware chromatography columns with an internal diameter of 13.4 mm and a reservoir capacity of 250 ml. Spikes of tritium, as a conservative tracer, were injected along with spikes of ^{233}U, as a reactive tracer, to assess fast-acting kinetics and compare the results for retardation generated in batch studies to those generated in column studies. Full elution time for the tritium injected in these columns was approximately 150 seconds.

Column studies were also performed to assess the accuracy of the multisite non-equilibrium reactive transport model developed. The columns were chromatography Flex Columns from KONTES. For kinetics reasons discussed in Section 3.3, a small volume column was used and can be seen adjacent to the purple-capped PP centrifuge tube in Figure 2.2. The column was connected to an NE-300 Syringe pump to permit a constant injection of solution. The syringe pump was used as initial experiments used gravity fed column flow but the flow rate, even in a small diameter column, was still too fast to adequately measure retardation in the uranium flow. Tritium was used as both a conservative tracer during the validation experiment and was used to measure the effective dispersion coefficient (D) of the column. Conclusions about the retardation behavior of uranium were then generated by comparison to the tritium flow data. A picture of the experimental set-up is shown as Figure 4.4.

2.7 Computer Assisted Methods

CXTFIT

CXTFIT is a code included in the STudio of ANalytial MODels (STANMOD) public domain software originally developed by researchers at the Colorado School of Mines. It solves the differential convection-dispersion equation shown below in equation 2.1. This version neglects both production and decay. As the half-life of uranium is extremely long relative to our modeling time period, decay was neglected as a conservative assumption. Production was neglected due to the ability to superimpose transportation curves with each other.

$$\frac{d}{dt}(\theta c_r + \rho s) = \frac{d}{dx}\left(\theta D \frac{dc_r}{dx} - J_w c\right) \qquad Equation\ 2.1$$

Where,
J_w = Solution Flux
D = Dispersion Coefficient, L^2/T
ρ = dry bulk density of graphite in column M/L^3
θ = volumetric water content L^3/L^3
X= distance, L
t = Time, T
c_r = resident concentration, M/L^3
s = concentration sorbed phase, M/M
Note, $s = K_d c_r$

If steady-state flow is assumed Equation 2.1 reduces to Equation 2.2

$$R\frac{dc_r}{dt} = D\frac{d^2c_r}{dx^2} - v\frac{dc_r}{dx} \qquad Equation\ 2.2$$

Where,
R = retardation factor, dimensionless
v = pore-water velocity, L/T

As differences in retardation for heavy metals have been noted when comparing results generated from batch studies and column studies, this program can be used to examine the validity of applying batch results to column

results. In addition, the eventual model proposed for reactive transport of uranium through a graphite matrix was validated by predicting the results from column experiments detailed above and then comparing the predicted results to the actual measured results.

CHAPTER 3

RESULTS

3.1 Characterization of Graphite

3.1.1 Physical Properties

Phase

The Alfa Aesar graphite used experimentally was characterized without difficulty by Powder X-Ray Diffraction. Results of the XRD analysis are shown below in Figure 3.1.

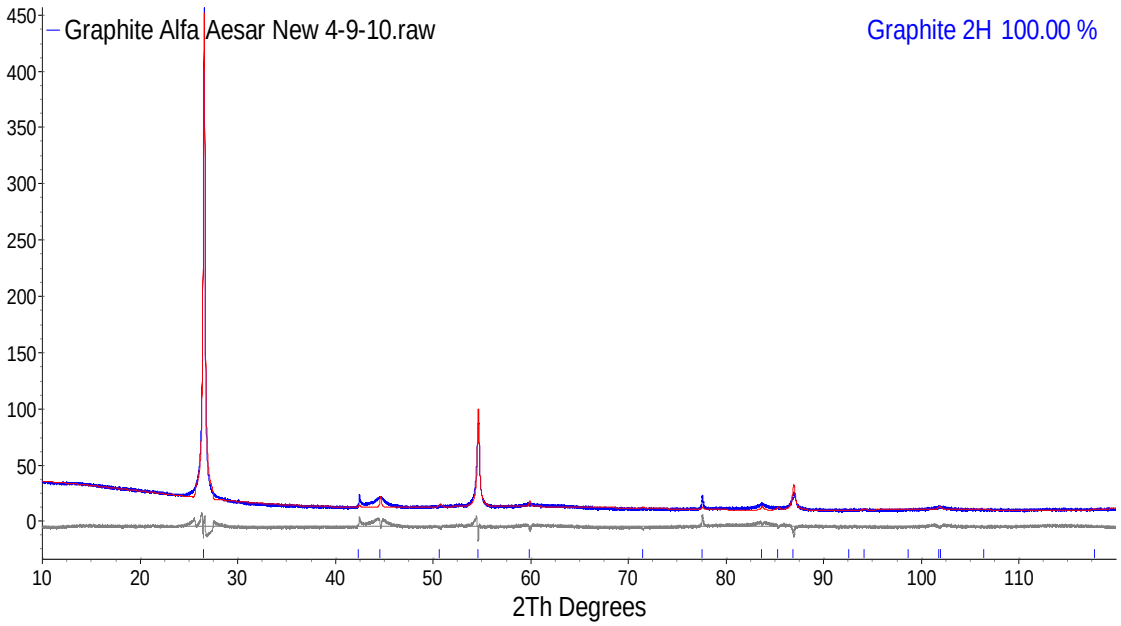

Figure 3.1: Powder X-ray Diffraction Analysis of experimental graphite with Topas comparison

Bruker's Topas software with the EVA database was used to compare the experimental results with known XRD spectra for graphite. (The theoretical pattern is the red color shown in Figure 3.1 and the blue color underneath is the experimental data. The gray line underneath indicates the differences between

the theoretical expected pattern and the measured pattern.) As discussed in Section 2.3, the presence of other graphite species could potentially prejudice batch sorption results in an unpredictable fashion. The results indicate pure phase graphite to the detection limits of the Bruker XRD device used in this analysis and are a strong indication that the graphite used was monophasic.

Functionalization

Surface functionalization of the experimental graphite was examined using infrared spectroscopy as outlined in Section 2.3. Graphite has been previously studied using this technique and data in the literature is available on the intrinsic infrared spectra of graphite. Results of the IR analysis are shown below in Figure 3.2.

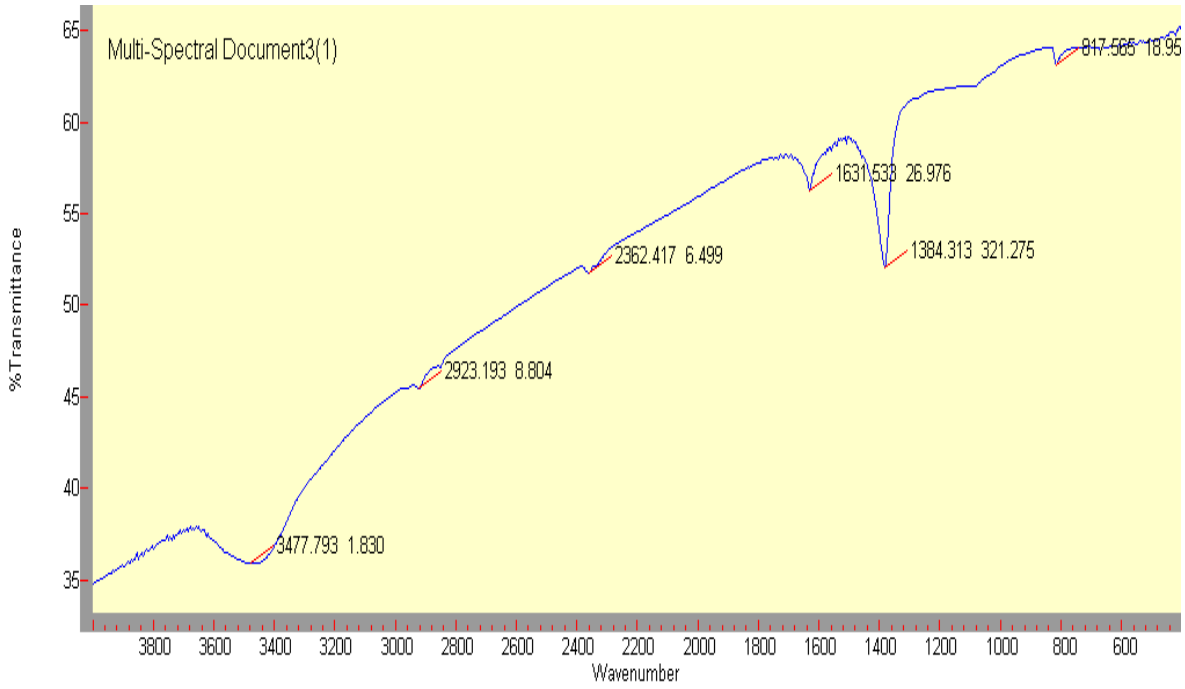

Figure 3.2: Infrared Spectra of Experimental Graphite

The IR results (wavenumbers of stretches) are shown below compared to expected data from the literature (Friedel & Carlson, 1971) in Table 3.1.

Expected Peaks, cm^{-1}	Measured Peaks, cm^{-1}
1587	1631
1362	1384
830 (weak)	817
2200 (weak)	2362
N/A	3477
N/A	2923

Table 3.1: Experimental IR peak comparison to literature data

For the four expected peaks from a spectra of pure graphite, there is good experimental agreement with expected results. There are also two additional peaks in the experimental spectra that were investigated. The stretch at a wavenumber of 3477 has been identified in the literature as a combination peak of hydroxyl groups on the graphite surface and water molecules that are most likely from the air (Mermoux *et al*., 1991). The weakest stretch that could be reasonably isolated occurred at a wavenumber of 2923 and could potentially be indicative of methyl group formation on the graphite surface as C-H groups would be expected at an approximate wavenumber of 3000 (Stuart, 2004). The source of these methyl groups remains unknown. Implications of this IR structure of graphite with regards to surface chemistry and complexation models will be discussed in Section 4.1.

Surface Area

The experimental graphite was characterized by BET Surface Analysis as well with the results being shown below in Table 3.2. The results from the

Quantachrome Silicon Nitride standard (Nominal SSA = 0.507 ± 0.085 m^2/g) run to assess experimental error are also shown.

	Specific Surface Area (m^2/g)	
	Graphite	Quantachrome standard
Sample Run 1	0.5310	0.5204
Sample Run 2	0.5335	0.5341
Sample Run 3	0.5987	0.5208

Table 3.2: Specific Surface Area measurements of Graphite and Quantachrome Standard

To quantify repeatability of the experiment the same Quantachrome Standard was run consecutively five times to determine experimental consistency and this data is shown below in Table 3.3.

Sample Run	Specific Surface Area (m^2/g)
#1	0.5204
#2	0.5057
#3	0.3668
#4	0.4945
#5	0.5225

Table 3.3: Repeated Surface Area Measurements of Same Quantachrome Standard

The average of the specific surface area measurements taken of the experimental graphite was 0.5544 ± 0.0274 m^2/g with an error obtained from comparing the measured results from the Quantachrome standard to its calibrated surface area.

3.1.2 Electronic Properties

Proton Exchange Capacity

The PEC of the experimental graphite was measured by potentiometric titration as described in section 2.3. A typical titration is shown below in Figure 3.3. The difference used to calculate the PEC is most pronounced on the upward titration on the right side of Figure 3.3. The shape of the curve does not indicate any discontinuities over the titration range indicating that PEC stays relatively constant with changing pH. The largest experimental variability was noted in the near-neutral region due to the sensitivity of the measuring system to small changes in pH so the average PEC was calculated in the pH region between 2.5 and 4.0 with a result of 0.25 ± 0.15 millieq /100 g of graphite. Combined with the specific surface area measurements of graphite this yields a specific exchange of 451 ± 91 μmoles H^+ / m^2 of graphite surface.

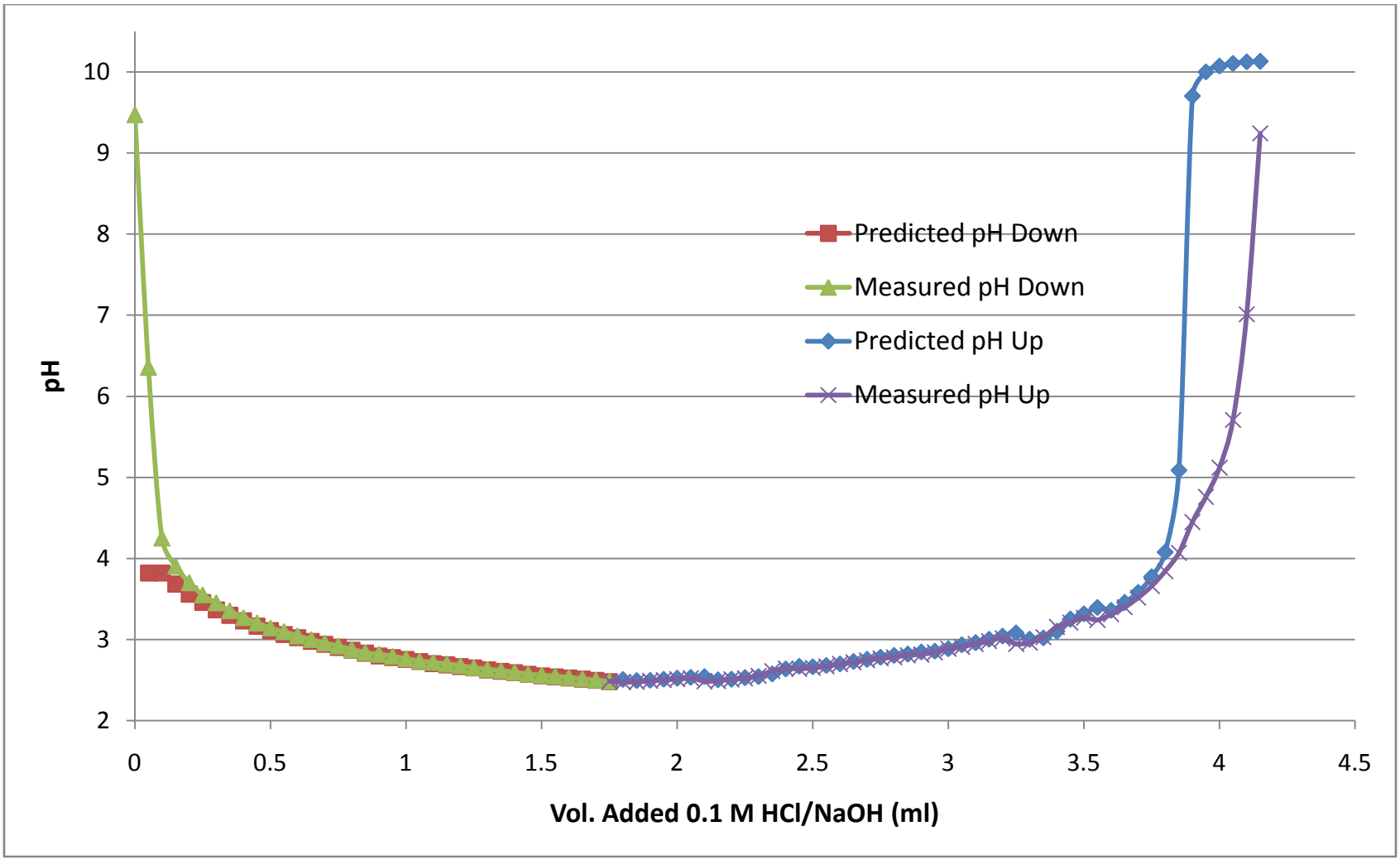

Figure 3.3: Sample Potentiometric titration of graphite (Color change indicates change from acid to base addition)

Point of Zero Charge

The net results of titrations performed to establish the point of zero surface charge for the graphite are shown below in Figure 3.4.

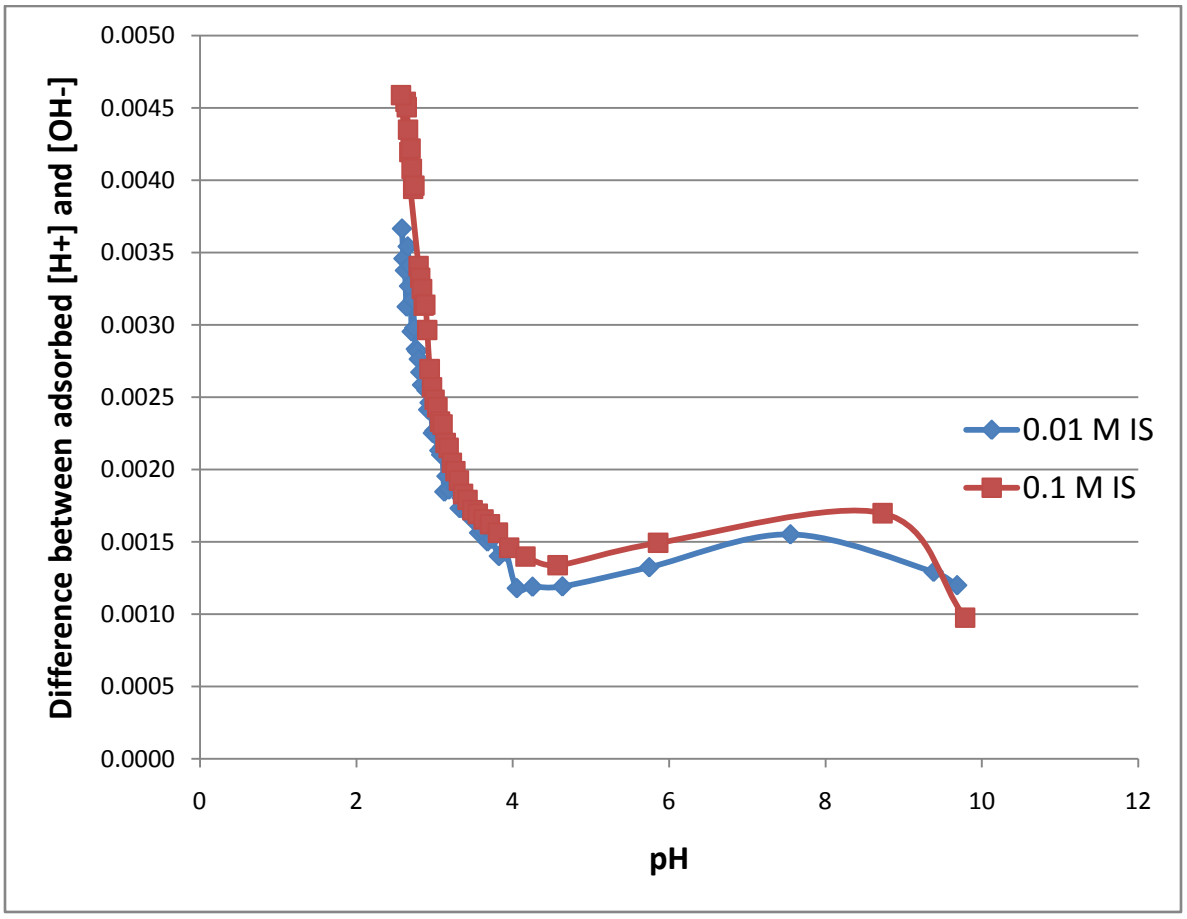

Figure 3.4: Titrations of graphite under different ionic strength

The two titration curves cross at pH ≈ 9.3. The deviation from the trend noticed in the neutral region is yet unexplained and cannot be accounted for. It is reported as a real effect because it was seen in all titrations done but the most likely answer is experimental error in a region that is very sensitive to small changes in pH. Correspondingly, the equations used to calculate the difference in

surface charge concentrations are also affected. The literature has reported data for the PZC of graphite with a significant variance ranging from acidic to alkaline values for graphite electrodes and treated graphite powders respectively (Golub *et al*., 1989, Sunwoo *et al.*, 2000). This data is in agreement with the range of PZC values discussed in the literature and it appears that the PZC of graphite is both sensitive to the treatment method of the graphite as well as the electrolyte composition (Golub *et al.*, 1989).

3.2 Equilibrium Uranium Sorption

Initial Kinetics Results

The first experiments performed were designed to determine an appropriate contacting time for the equilibrium uranium/graphite sorption batch experiments. The first sorption experiment was performed at pH = 5 and 0.5, 5, 25 and 50 ppm uranium solution concentrations. Samples were taken at a period starting after five days equilibration and continuing to 60 days of equilibration. Initial and final results are shown below in Table 3.4.

	Mass % Uranium in Solution Sorbed	
Sample Conc. (ppm)	5 Day	60 Day
50	6.74% ± 1.1%	6.97% ± 2.5%
25	10.4% ± 2.5%	11.8% ± 2.6%
5	35.5% ± 5.4%	42.1% ± 4.8%
0.5	82.0% ± 5.0%	85.1% ± 3.3%

Table 3.4: Kinetics data for change in uranium solution concentration over time

All changes over the additional contacting time were within the margins of error and intermediate sampling showed no deviations. As a result, for all batch

experiments where an equilibrium measurement was desired contacting time was fixed to at least 5 days.

Equilibrium Uranium Sorption

Scoping work was begun at mass levels of uranium as high as 1000 ppm but preliminary results suggested that the range of interest for uranium sorption was significantly lower. The lowest mass concentration used at all pH points for uranium sorption was 500 ppb uranium ([U] = 2.1 X 10^{-6} M). This point was chosen to represent an elevated uranium concentration that would be high for a groundwater plume but within the expected region for a TRISO fuel compact. Batch equilibration experiments were performed systematically at mass levels as high as 50 ppm to represent an upper boundary of a uranium plume. A graph of uranium sorption to graphite as a function of pH with [U] = 500 ppb under atmospheric CO_2 and ionic strength = 0.01 M NaCl is shown below in Figure 3.5.

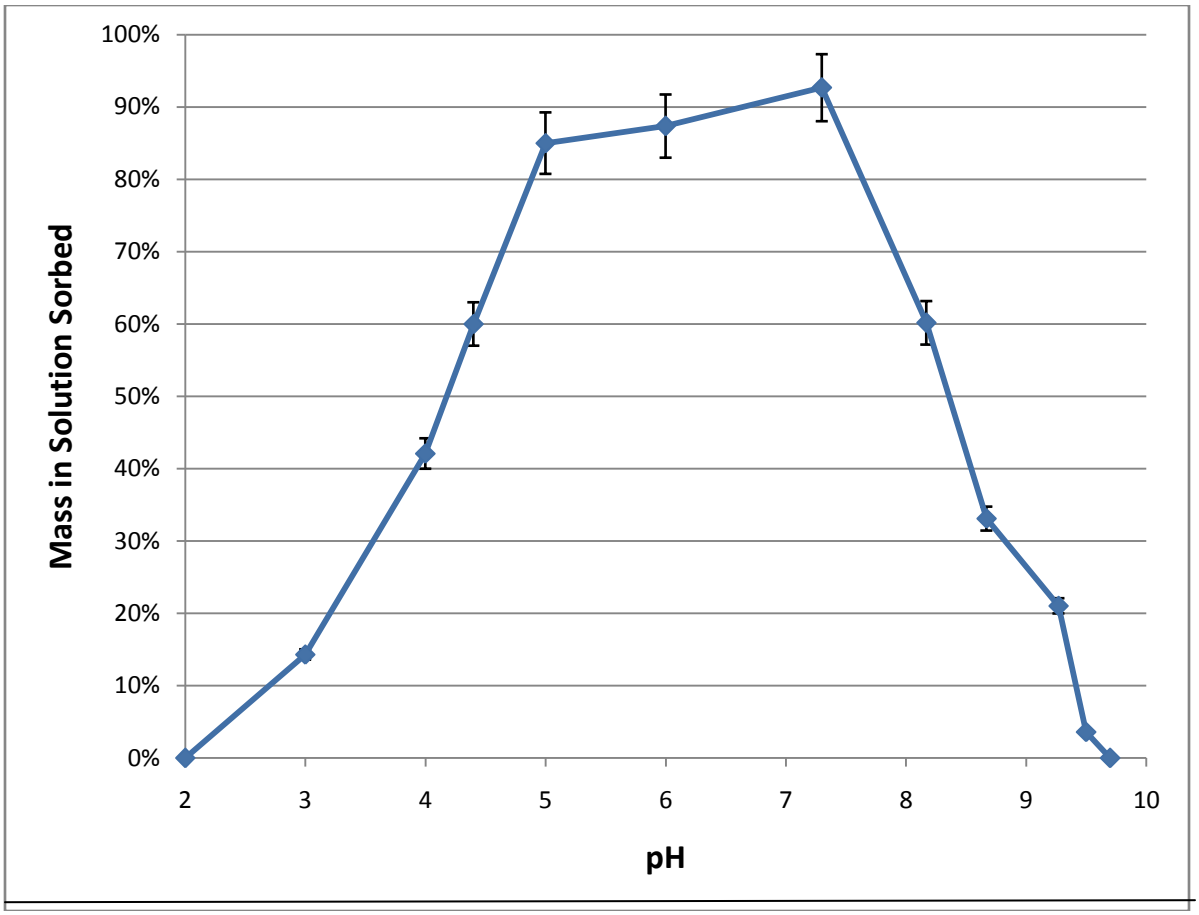

Figure 3.5: Uranium sorption (Initial [U] = 500 ppb) to graphite as a function of pH Ionic Strength = 0.01 M, pCO_2 = 390 ppm

Uranium sorption was found to be significant in the region between pH = 2 and pH = 9.5. Maximum values for uranium sorption to graphite are observed in the near neutral region: rising to maximum experimental value at pH = 7.3 with 92.6% ± 0.97% of the uranium in solution sorbed. K_d also shows significant variation with pH which is shown below in Figure 3.6.

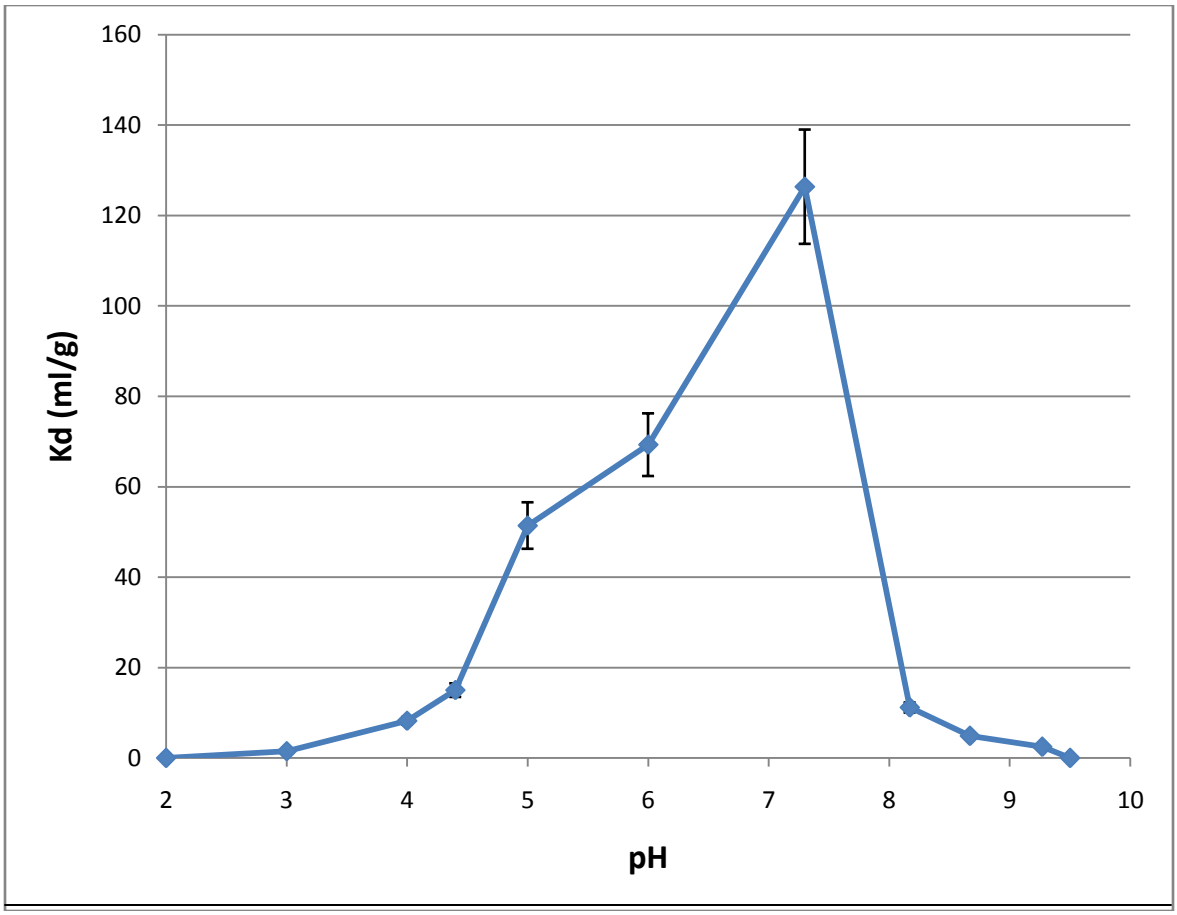

Figure 3.6: Variation in Kd with pH (Initial [U] = 500ppb)

Using Equation 1.4 to calculate a conservative estimate of the retardation factor for a 500 ppb uranium solution moving through a graphite matrix gives the results shown below in Table 3.5.

pH	Kd (ml/g)	Retardation factor
3.00	1.5 ± 0.13	16.3 ± 2.32
4.00	8.2 ± 0.68	83.3 ± 7.79
4.40	15.0 ± 1.39	151.3 ± 14.91
5.00	51.4 ± 0.54	515.3 ± 6.40
6.00	69.3 ± 4.98	694.1 ± 50.78
7.30	126.4 ± 7.03	1264.6 ± 71.29
8.17	11.2 ± 1.18	112.8 ± 12.76
8.67	4.9 ± 0.45	49.9 ± 5.48
9.27	2.5 ± 0.25	25.8 ± 3.47

Table 3.5: Sample retardation coefficients for aqueous uranium in graphite

Effects of CO_2 Partial Pressure on Sorption

With pH held constant at approximately 9.3 by a Borax buffer as described in Section 2.2, uranium sorption to graphite was evaluated under different partial pressures of CO_2 ranging from less than 1 ppm to a saturated CO_2 atmosphere. The results from the experiments are shown below in Table 3.6.

$[CO_2]$, ppm	pH	Mass % Sorbed	K_d (ml/g)
Atmospheric	9.27	21.0% ± 2.27%	2.48 ± 0.25
< 1	9.30	36.7% ± 2.11%	5.48 ± 0.28
~1,000,000	9.28	~0%	N/A
~1,000,000	7.5	~0%	N/A

Table 3.6: pH Results for sorption experiments under varying CO2

The results from experiments performed under acidic conditions with normal acid/base pH adjustment under varying partial pressures of CO_2 are shown below in Table 3.7.

$[CO_2]$, ppm	pH	Mass % Sorbed	K_d (ml/g)
Atmospheric	4.85	75.3% ± 3.03%	39.3 ± 4.9
~1,000,000	4.75	28.78% ± 6.59%	4.43 ± 1.6

Table 3.7: pH Results for sorption experiments under varying CO_2

Implications arising from these results will be discussed in Section 4.

Effects of Ionic Strength on Uranium Sorption to Graphite

The experimental methodology used for the elevated salt concentrations ([NaCl] > 0.1 molal) was described in Section 2. The effect of increased ionic strength through the addition of NaCl is shown below in Table 3.8. These results all used a uranium concentration of 2.1 μmolal under atmospheric CO_2.

pH	[NaCl] (molal)	K_d (ml/g)
4.03	0.01	8.23 ± 0.08
4.06	0.05	8.58 ± 0.04
4.07	0.1	7.73 ± 0.05
5.07	0.01	51.43 ± 6.84
5.14	1	58.74 ± 15.5
5.16	4	59.84 ± 19.5

Table 3.8: Kd variation with ionic strength

Effect of Uranium metal concentration on sorption

Uranium metal concentration in solution strongly affects equilibrium uranium partitioning to graphite (as shown by variance in K_d). Sorption isotherms are shown below in Figure 3.7.

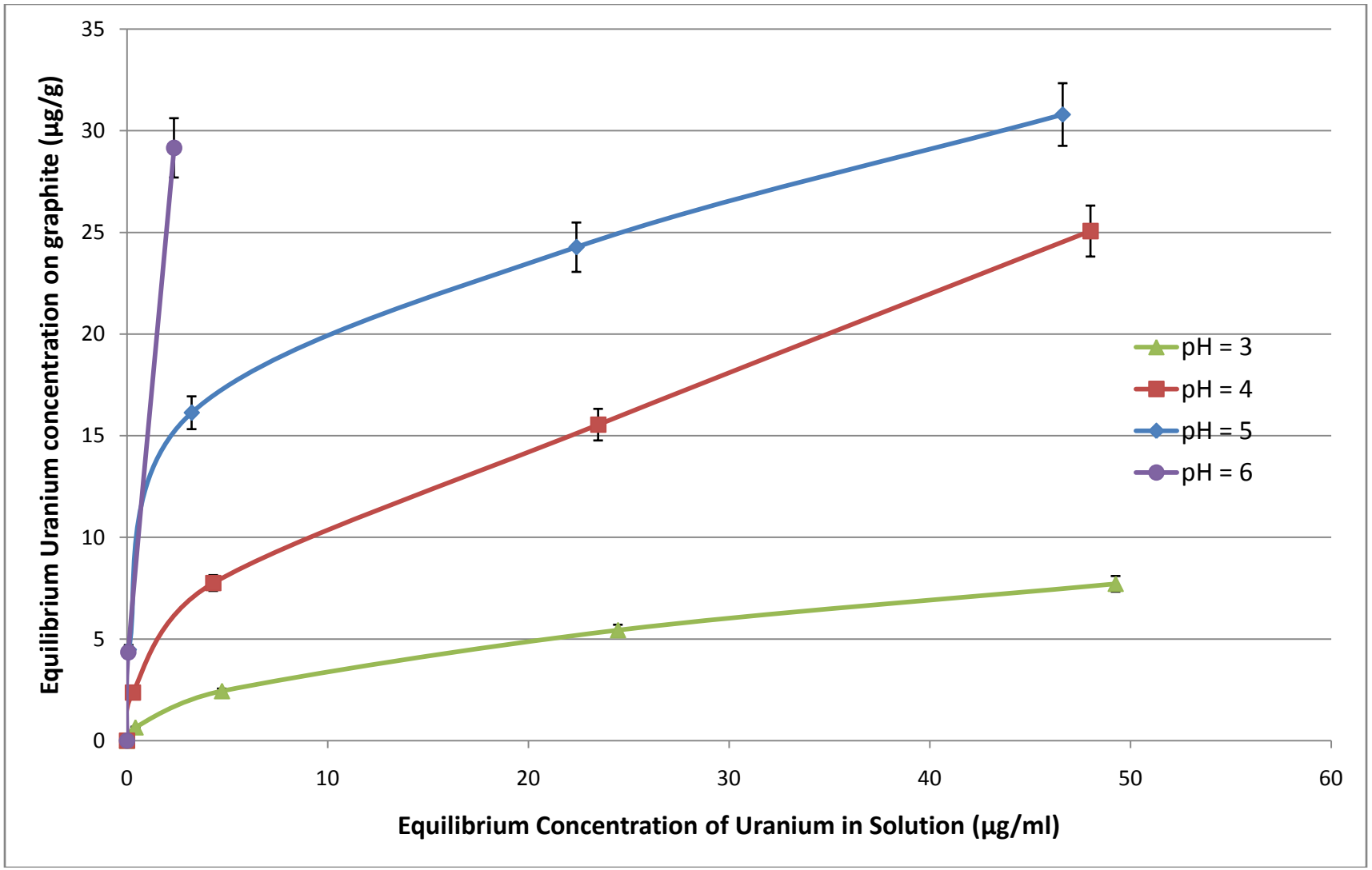

Figure 3.7: Equilibrium sorption isotherms for uranium sorption to graphite

These data indicate a strong relationship between equilibrium uranium solution concentration and concentration of uranium on the graphite surface. It was also noted that a precipitate was formed at pH 6 for both the 25 and 50 ppm uranium solutions used in these experiments. This precipitate is why the pH = 6 curve shown above is not identical to the other sorption isotherms shown. Speciation results from EQ 3/6 suggest that at this mass concentration the equilibrium solid species precipitating should be schoepite $[(UO_2)_4O(OH)_6 \cdot 6(H_2O)]$. This precipitate was analyzed by powder XRD. The results of the XRD analysis are shown below in Figure 3.8.

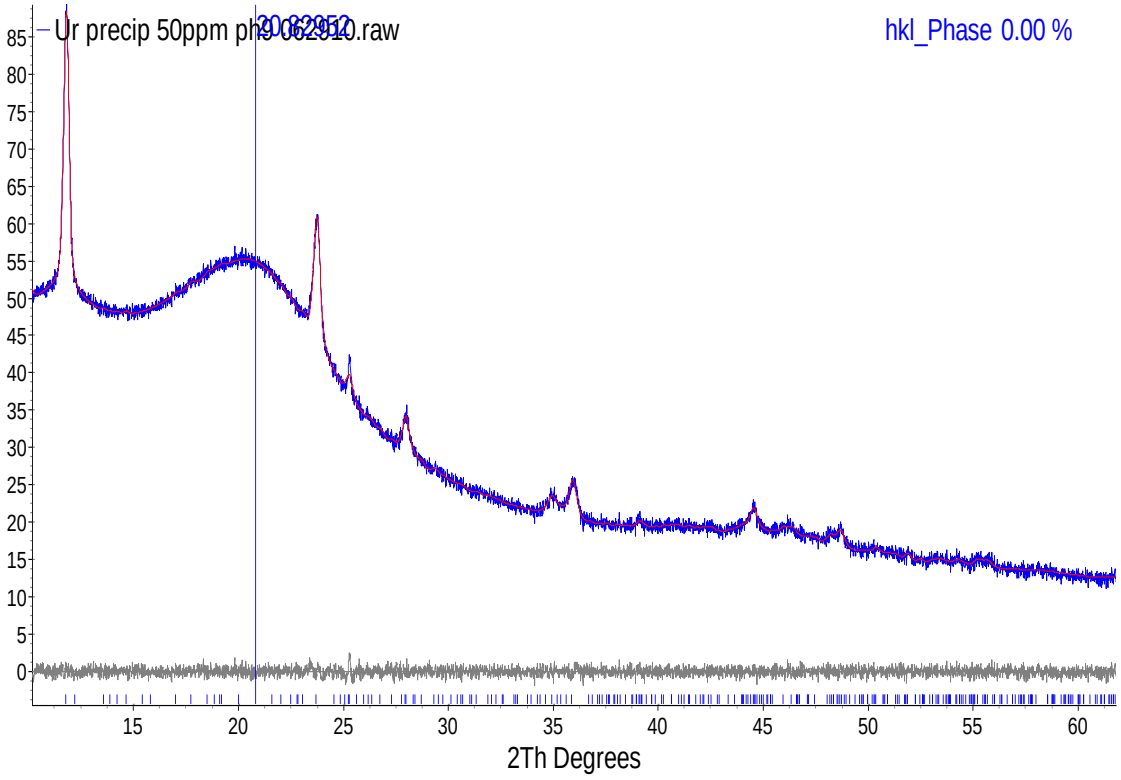

Figure 3.8: 50 ppm pH = 6 Precipitate XRD Analysis

These XRD results are consistent with the formation of a sodium meta-schoepite species. This indicates that the NaCl used to control ionic strength is

participating in aqueous reactions above a certain uranium concentration. Additionally, it indicates that in the experimental time frame used, kinetic effects are more important for solid precipitation from solution than the calculated results at equilibrium. For the neutral and alkaline pH region, mass concentrations of uranium in solution were reduced to avoid the formation of precipitates.

The sorption isotherms appear to follow L-shaped isotherms as described in Section 1.2.2. The two most common adsorption isotherms used for evaluating L-shaped sorption isotherms are the Langmuir isotherm and the Freundlich isotherm. The equations are shown below as Equations 3.1 and 3.2, respectively.

$$q = \frac{bK_L c_{eq}}{(1 + K_L c_{eq})} \qquad Equation\ 3.1$$

Where,
q = Mass uranium sorbed per mass graphite, µg/g
c_{eq} = Conc. of solution after equilibration, µg/ml
K_L = Empirical Langmuir parameter, ml/g
b = Empirical parameter, usually indicated as adsorption maxima, µg/g

$$q = K_F c_{eq}^N \qquad Equation\ 3.2$$

Where,
q = Mass uranium sorbed per mass graphite, µg/g
c_{eq} = Conc. of solution after equilibration, µg/ml
K_F = Empirical Freundlich parameter, ml/g
N = Empirical Freundlich parameter, dimensionless

Both Langmuir and Freundlich isotherms were evaluated for their fit to the experimental data using pH = 5 data as a representative data set. These data are shown below in Table 3.9. (Note: This requires several trivial linear transformations. Details can be found in Essington, 2003)

Initial Uranium Conc. (ppm)	Eq. Uranium Conc. (ppm)	q (µg/g)
0.1	0.0033	0.83
0.5	0.09	4.48
5	3.23	16.13
25	22.40	24.27
50	46.63	30.79

Table 3.9: pH = 5 Data used for isotherm fitting

The results of the Langmuir fit and a plot of the statistical residuals are shown below in Figures 3.9 and 3.10, respectively. There is a high correlation coefficient between the transformed Langmuir equation and the experimental data at pH = 5 with an R^2 value of 0.984. This is a high R^2 value indicating that a Langmuir fit does describe the data well. However, the plot of the statistical residuals for the Langmuir fit shows a strong curvature indicating that while there is a high R^2 value it is perhaps not the best method of describing the experimental data. The Langmuir method also requires certain assumptions about sorption behavior to be justified which are not necessarily so in this case. This will be discussed in further detail in Section 4.

A Freundlich isotherm was fit to the data next. This fit was also successful in describing the data with an R^2 value of 0.98. In addition, the residuals plot of the Freundlich transformed data shows residuals that are evenly spaced about the prediction equation without the marked increase and decrease apparent in the Langmuir data. This indicates that a Freundlich fit, shown as Equation 3.3, is appropriate for the data.

$$q = K_F c_{eq}^N = 0.930\ c_{eq}^{0.37} \qquad Equation\ 3.3$$

Where, terms are as defined above

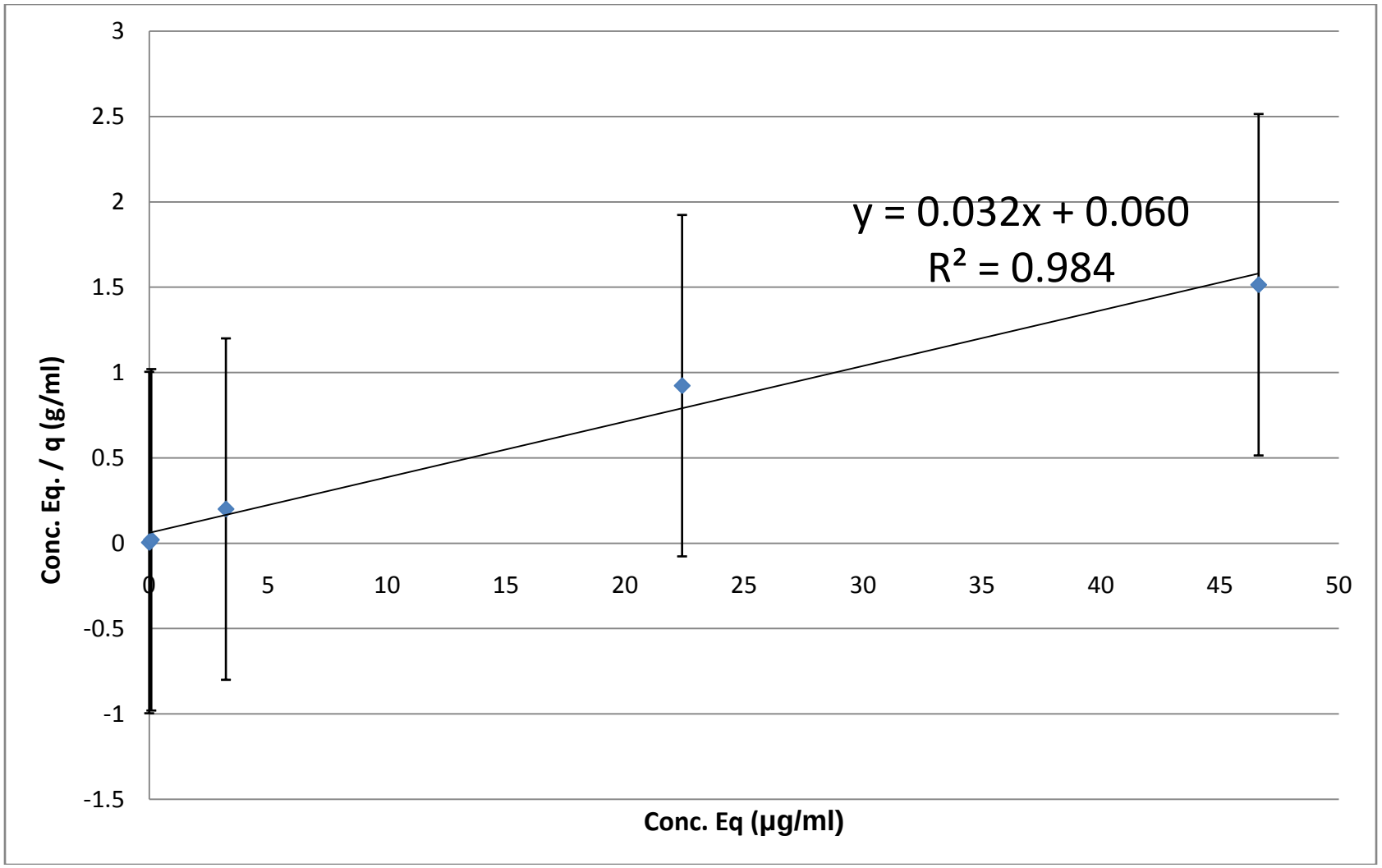

Figure 3.9: Langmuir fit of sorption data for pH = 5 with regression equation (slope = 1/b, intercept = 1/bK$_L$)

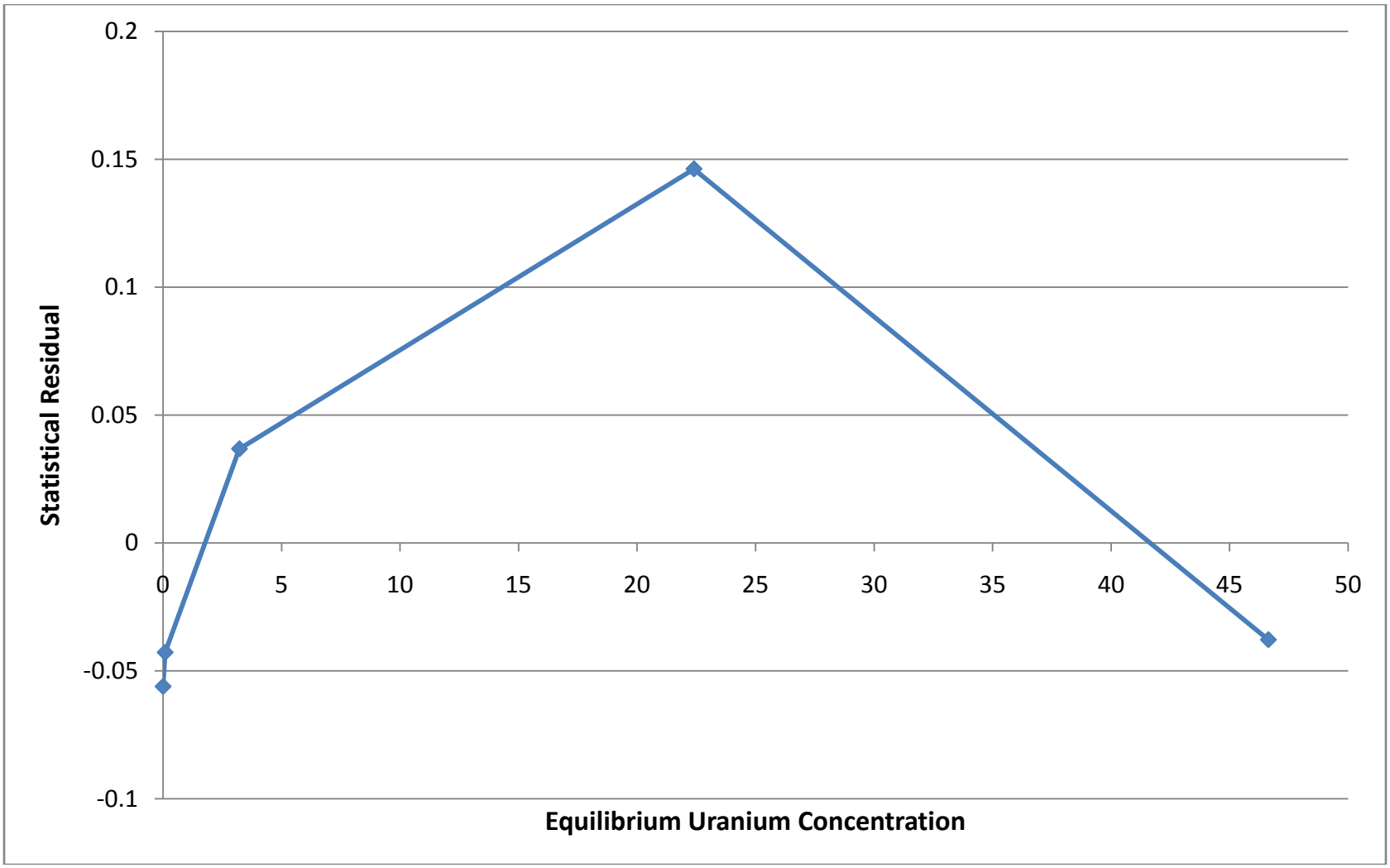

Figure 3.10: Residuals for Langmuir fit of Sorption data at pH = 5

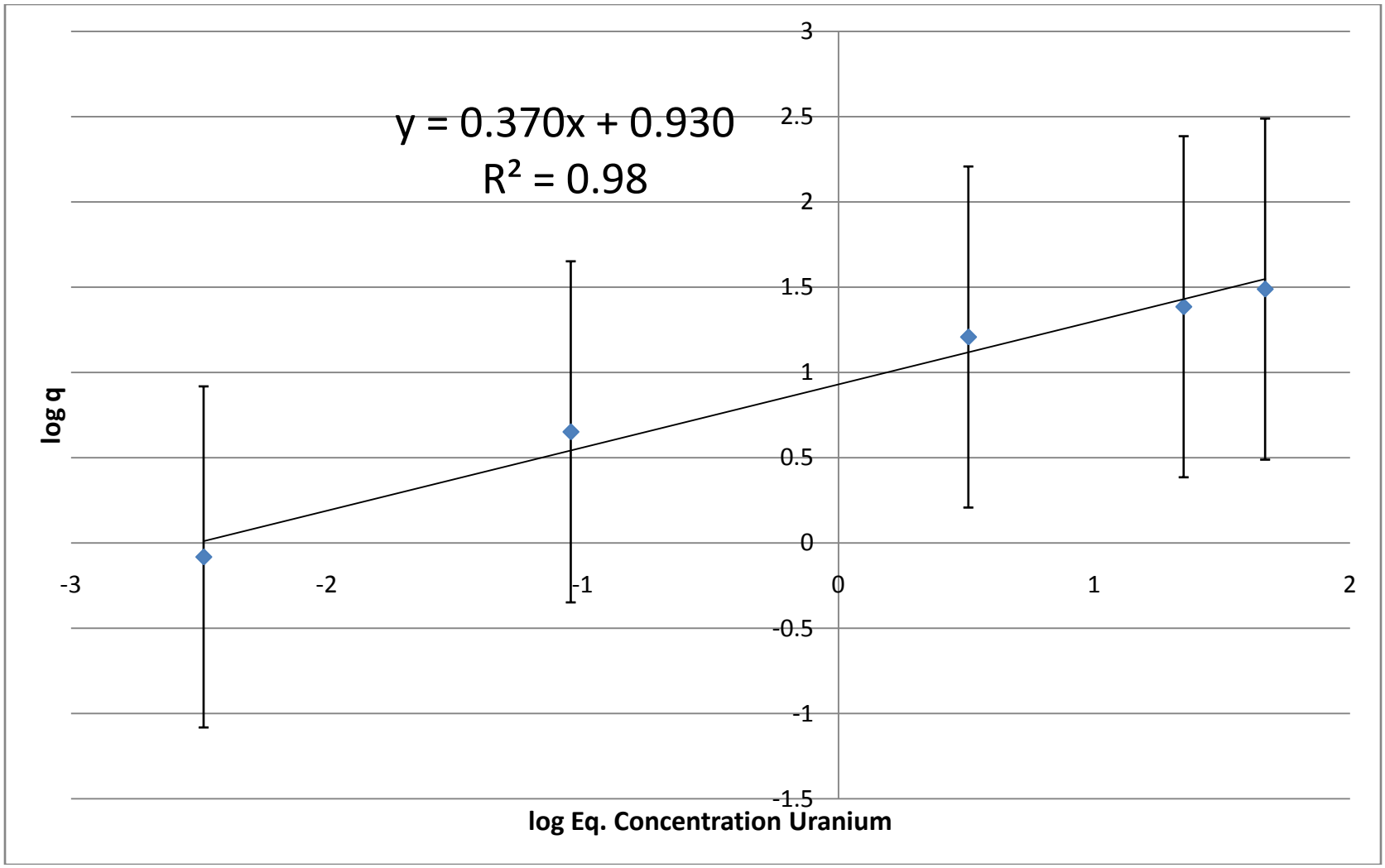

Figure 3.11: Freundlich Fit to pH = 5 sorption data (slope = N, intercept = K_F)

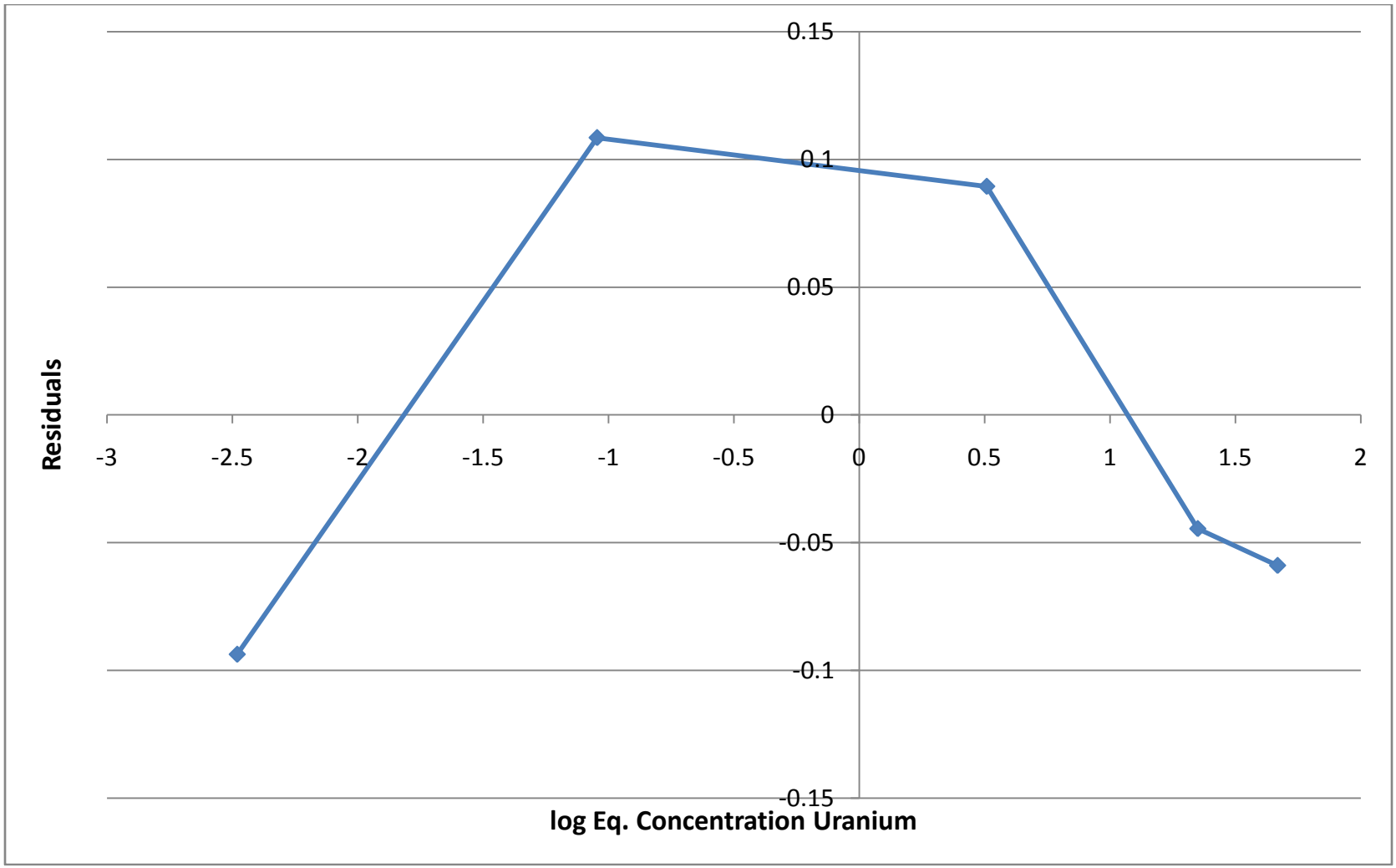

Figure 3.12: Statistical Residuals of Freundlich fit to data

3.3 Kinetics Results

Batch Kinetics Results

The initial kinetics experiments that were performed to measure an appropriate equilibration time for uranium/graphite mixing were then performed with a shorter initial sampling interval to examine the linearity of the kinetic phase of uranium sorption to graphite. Data from these experiments are shown below as Figure 3.13.

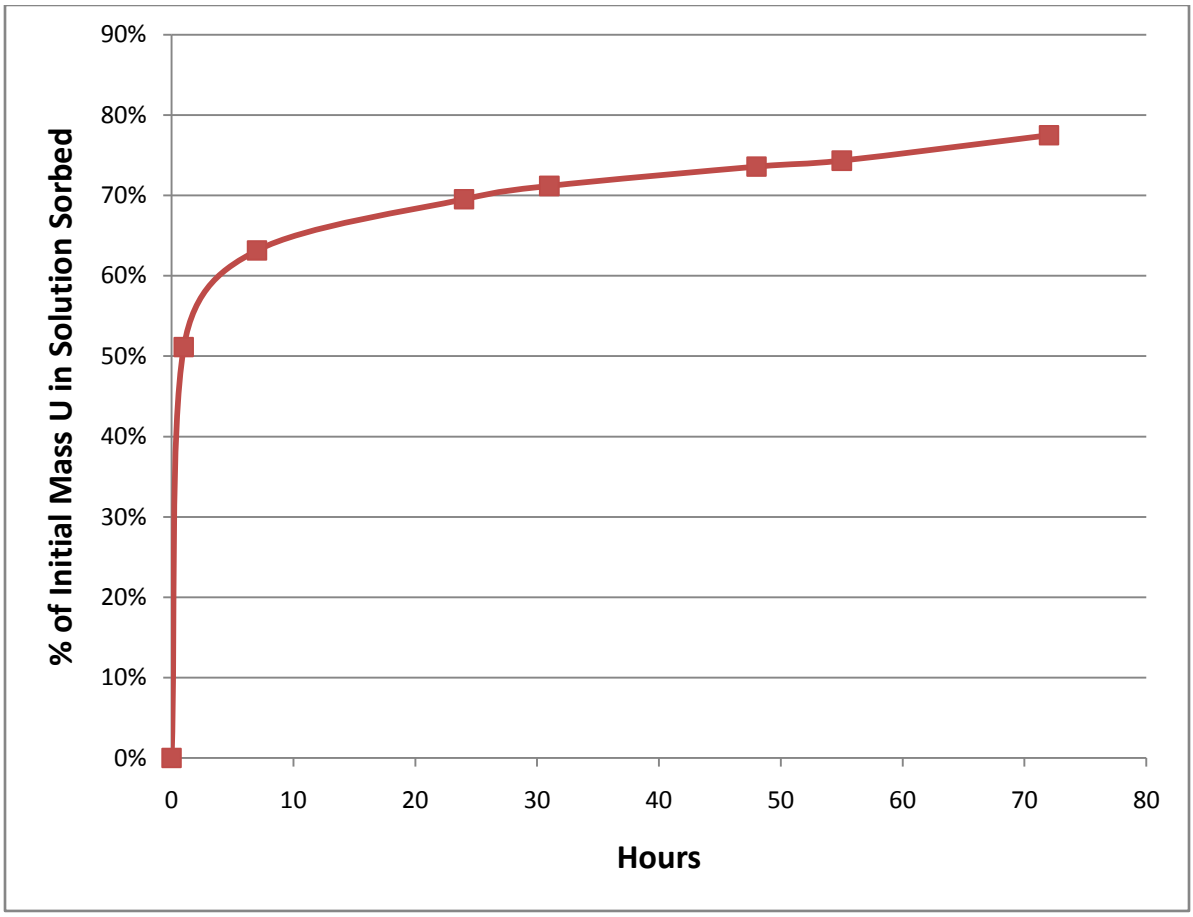

Figure 3.13: Sorption data with an initial sampling time of one hour, [U] = 500 ppb, pH = 5

The rapid sorption during the first hour of contacting necessitated experiments with even shorter sampling intervals in the minute range. After vigorous shaking with a solution contacting time of one minute, 49.9% ± 5.5% of the aqueous uranium was observed to be sorbed to the graphite. There is no significant difference between this value and the observed value shown above for sorption after one hour of contact time of 51.1% ± 4.8%. This indicates that at the 500 ppb level at pH = 5 approximately 50% of the uranium in solution immediately sorbs to the graphite. Batch results indicate that 82.0% ± 4.96% of the uranium in solution should sorb at this mass and pH. This indicates a strong non-linearity in kinetic response. After, the large initial fraction of uranium sorbs, approximately 72 hours were required before further changes in solution uranium concentration could not be noticed.

Fast Flow Column Experiments

Fast flow column experiments were performed with expected uranium contact times below that necessary for full equilibration between graphite and uranium in solution. The initial experiment injected 2 μg of ^{233}U along with an equivalent activity of tritium. Results are shown below in Figure 3.14.

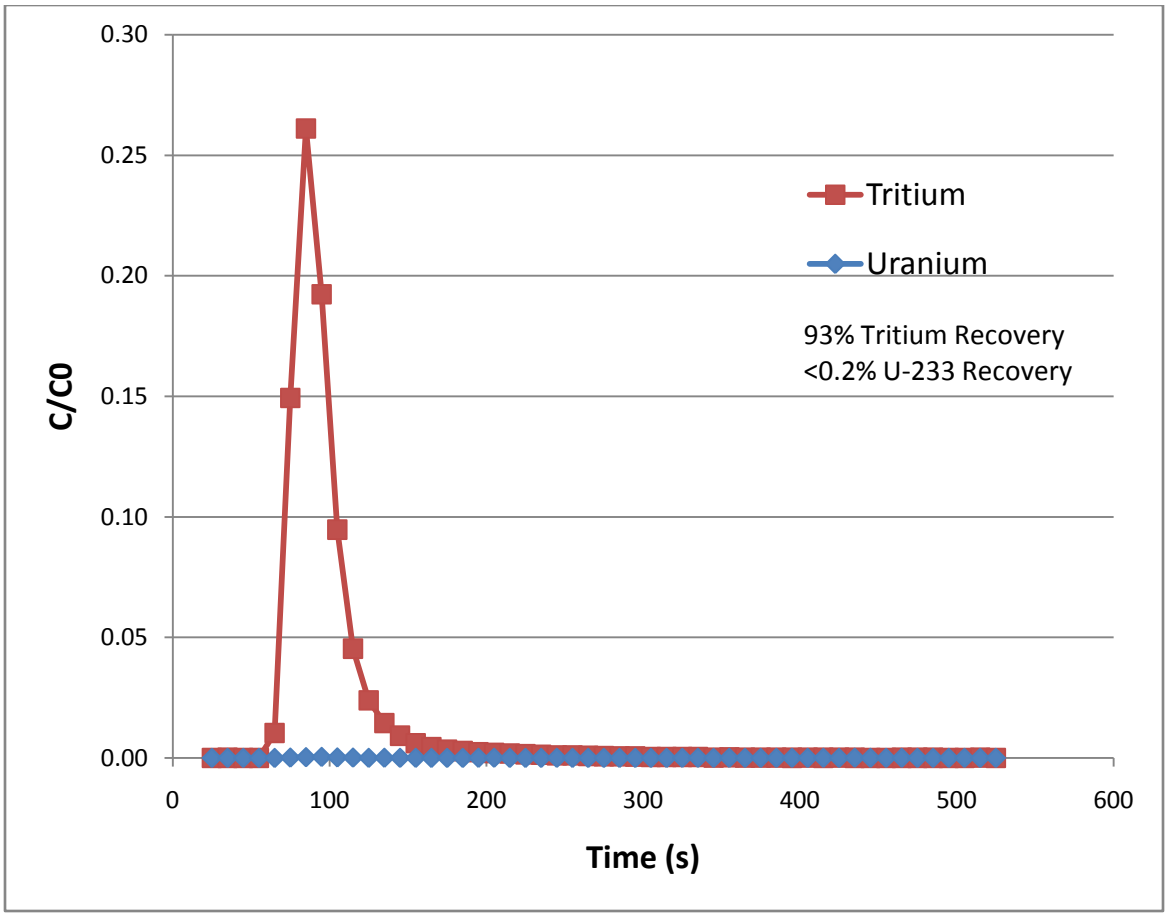

Figure 3.14: Initial Fast Flow Column Experiment (pH = 6.5) 2 µg U-233

The initial experiment resulted in near-complete recovery of the tritium used and nearly negligible recovery of the injected ^{233}U. As the columns were quite large, large amounts of graphite were used to influence the flow. To compensate for this, the amount of uranium used was increased to 16 µg. Results are shown below as Figure 3.15.

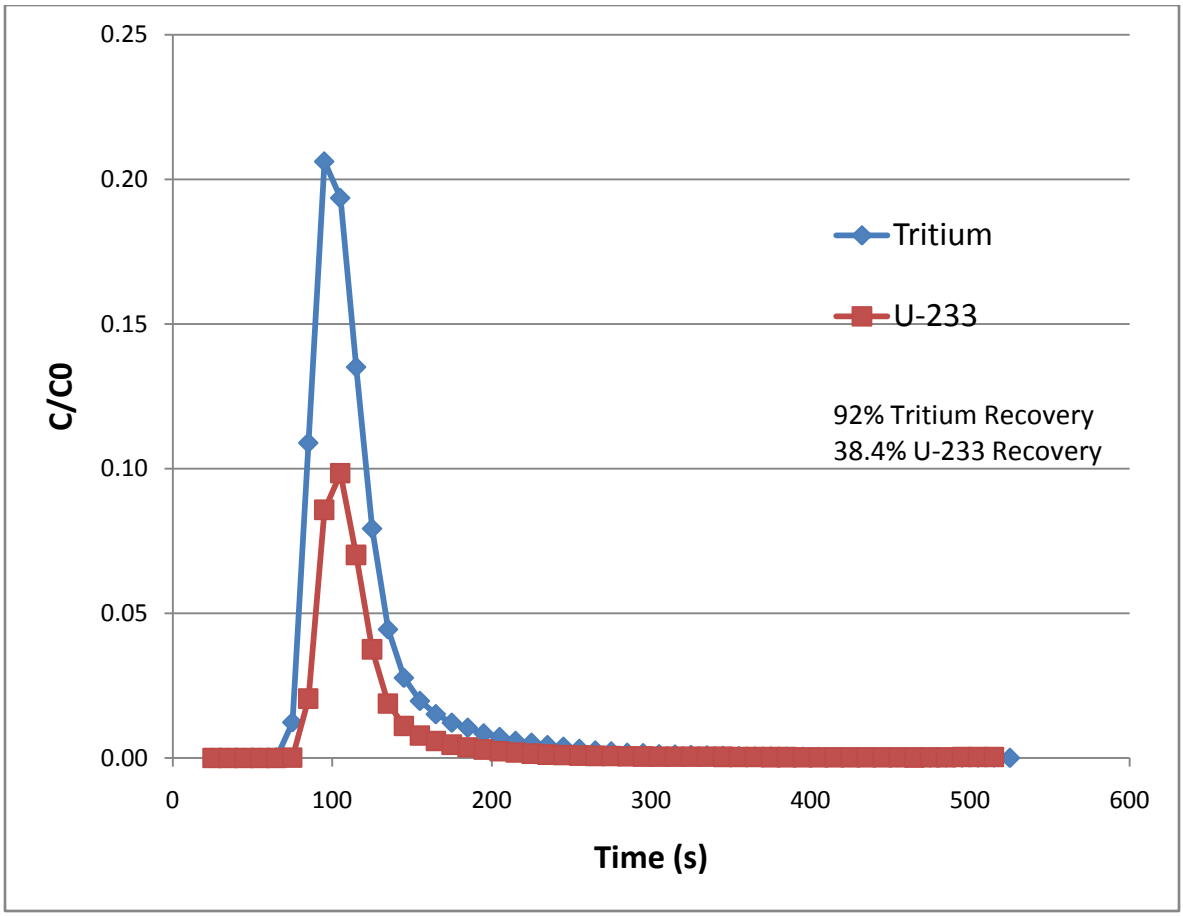

Figure 3.15: Fast Flow Column Experiment (pH = 6.5), 16 µg U-233

These results suggest certain details about the kinetics and nature of uranium partitioning to graphite that will be discussed in Section 4.

Section 3.4 Desorption

Batch Desorption Results

Batch desorption results with the procedure outlined in Section 2.4.2 are shown below for a contacting solution with pH = 5 and ionic strength = 0.01 M NaCl as Figure 3.16.

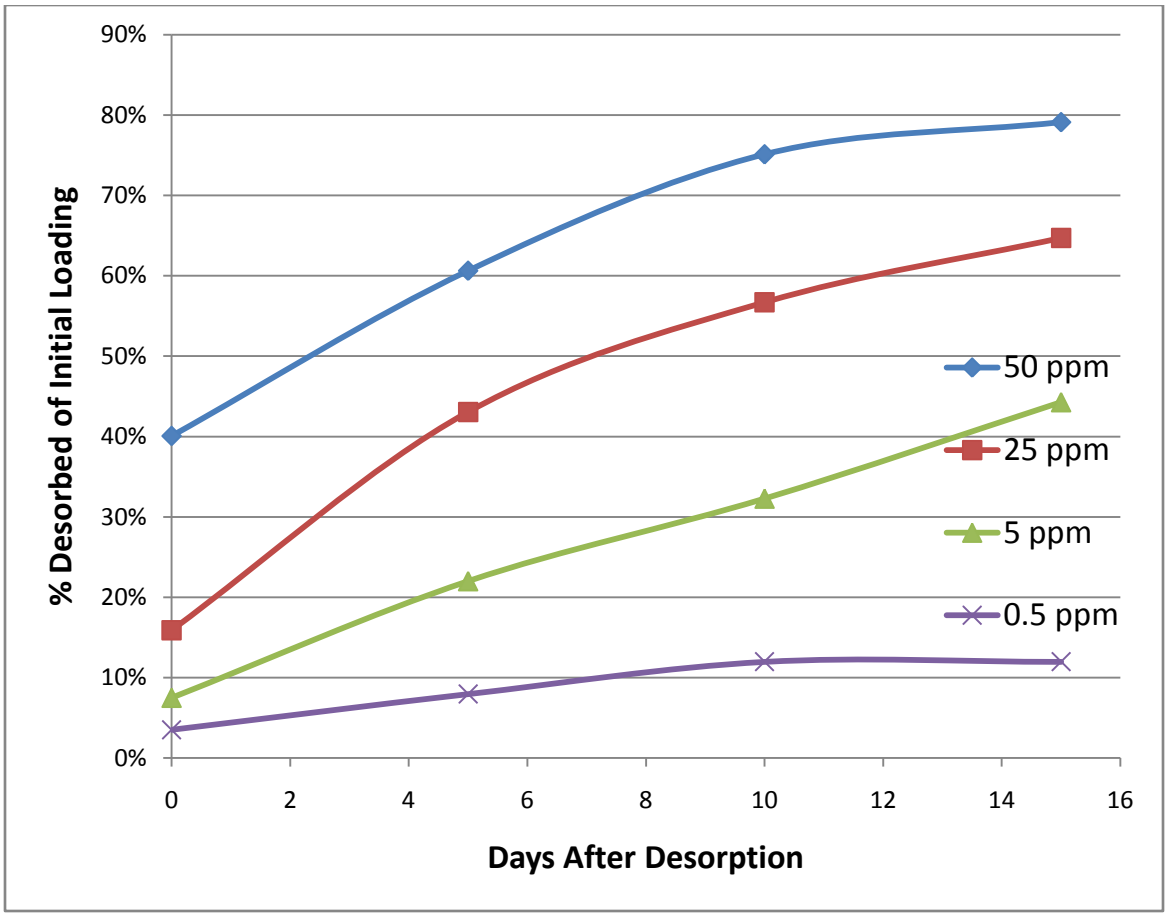

Figure 3.16: Batch Desorption Results for pH = 5 samples

The results indicate incomplete recovery of uranium in all the initial mass loadings studied. The average amount of uranium that remained sorbed after batch desorption is shown below in Table 3.10.

Initial [U] (ppm)	Percentage of U Desorbed	Mass U Remaining Sorbed (μg)
50	79.1% ± 8.1%	6.89 ± 0.55
25	64.7% ± 6.4%	7.96 ± 0.51
5	44.3% ± 7.8%	9.59 ± 0.75
0.5	12.0% ± 3.0%	3.14 ± 0.09

Table 3.10: Comparison of Desorbed U with Remaining Sorbed U Mass after Batch Desorption

These data indicate that, with the exception of the 500 ppb uranium level where relatively very little desorbed at all, there is good agreement to the mass of uranium that remains sorbed after batch desorption experiments were performed.

CHAPTER 4

DISCUSSION

4.1 Graphite Properties and Surface Chemistry

Electronic Structure

The graphite used experimentally in this work shows the ability to exchange charge in solution with a value of 0.25 ± 0.15 millieq /100 g of graphite. This value is shown compared to several other geologic materials of interest, as well as activated carbon, below in Table 4.1 along with a selected comparison of PZC for graphite as well (Activated carbon data from Kandah *et al.*, 2006, mineral and resin data from Langmuir, 1997).

Material	Exchange Capacity (meq/100 g)
Graphite	0.25 ± 0.15
Activated Carbon	154.5 - 191.2
Kaolinite	3 - 15
Zeolites	100-400
Synthetic Exchange Resins	290 – 1020

Table 4.1: Exchange Capacity Comparison

These results suggest that the graphite examined has a lower exchange capacity than most geological media as well as typical synthetic exchange resins. This is to be expected as in natural media such as soils the exchange capacity of the physical soil can be dominated by the presence of organic matter which has a significantly higher exchange capacity (Essington, 2003) and a resin manufactured for an exchange process would be expected to have significantly

higher performance than a natural material. The value for PEC reported is also several orders of magnitude lower than that reported for activated carbon in the literature. This also is not unexpected as activated carbon is known for being very reactive in solution and having a large capacity to exchange materials in solution (Langmuir, 1997). However, it should also be noted that the exchange capacity of the graphite used was higher than the amount of uranium present in solution so the exchange capacity does not appear to be a limiting factor in sorption.

The PZC reported for activated carbon in the literature is variable like that of graphite. However, the literature does indicate that during the process of activation through chemical and electrical means, the PZC will decrease in value (Kandah *et al.*, 2006). In a typical experiment in this work carbon activation lowered the PZC from pH = 4.2 to pH = 2.89. As this experimental work has shown that the PZC of the graphite used has a value of ~9.3, it is indicative that a large degree of activation has not taken place. However, as the IR work to be discussed below will indicate, the current graphite does show signs of activation. For future work, perhaps a measurement of PZC would be a way to quantify the degree of activation in a carbonaceous material. This would be of interest for pre and post irradiated nuclear graphite as a way to potentially analyze the activation that occurred during burn-up while requiring only small amounts of material for measurement.

Having established that graphite has the ability to both exchange charge in solution and that it will adsorb ions in solution, the question then becomes

what is the nature of this charge exchange? This requires further analysis of the physical characteristics and structure of the graphite

Physical Structure

The surface area measurements indicate that the graphite used has a lower surface area than many common geologic media as shown in Table 4.2 below.

Material	Specific Surface Area (m^2/g)
Graphite	0.507 ± 0.027
Activated Carbon	2217
Kaolinite	10 - 38
Montmorillonite	600 – 800
SiO_2 (Quartz)	0.14

Table 4.2: Comparison of Selected Surface Areas (AC data from Kandah et al., 2006 other data from Langmuir, 1997)

As can be seen above, the specific surface area measured for the experimental graphite is significantly below that of activated carbon and other representative geologic media and is more on the order of the crystalline quartz. Additionally, it can be noted that the specific surface area of activated carbon is four orders of magnitude above that for the experimental graphite. This suggests that both the large increase in surface area and exchange capacity during the activation process of carbon to activated carbon are at least partly responsible for the large increase in sorptive capacity observed between graphite and activated carbon.

The IR analysis of graphite has proven the most informative for understanding the mechanisms of surface adsorption between uranium in solution and the graphite surface. As most surface chemical adsorption reactions require the existence of a charge exchanging site and the capacity to exchange charge has been determined for the experimental graphite, it would be informative to be able to identify the mechanisms of that exchange. In Figure 3.2, the IR spectra of the experimental graphite was examined and obtained good agreement with the work of Friedel & Carlson in 1971 with the exceptions of peaks centered at wavenumbesr of 3477 and 2923. The peak located at a wavenumber of 2923 in the analysis is most likely indicative of methyl stretching (C-H bonds). It is unknown if these groups contribute to the ability of graphite to exchange charge but it is believed that they do not as the ability of a methyl group to protonate and deprotonate to exchange charge is limited. The peak centered at 3477 has been characterized in the study of graphite oxide as a combination peak of free hydroxyl groups (3544 cm^{-1}), hydrogen bonded hydroxyl groups on the surface (3400 cm^{-1}) and water molecules (3152 cm^{-1}) (Janowska *et al.*, 2010). The interpretation of the other four peaks observed and previously ascribed to graphite in the literature is summarized in Table 4.3 below.

Peak	Interpretation
1631	Stretching of C=C bonds
1384	Vibration of C-OH bonds
817 (weak)	Unknown
2362 (weak)	Unknown

Table 4.3: Interpretation of IR Data (Janowska et al., 2010)

It should be noted that while the nature of the two weak peaks at 817 cm^{-1} and 2362 cm^{-1} is unknown they have been previously identified in other IR spectra of graphite oxide (Bissessur *et al.*, 2006). This analysis combined with later work appears to suggest that the work of Friedel & Carlson on the characteristic IR spectra of graphite is incomplete and that what was actually measured in that case and in this case as well is a mixture of graphite and graphite oxide. As the structure of graphite consists of sp^2 hybridized bonds between carbon atoms, the characteristic stretch of graphite would appear to be the peak located at 1631 cm^{-1}. The peak at 1384 cm^{-1} is indicative of some C-OH bonds which would suggest that the protonation of these sites on the graphite surface are the sites of interest with regards to surface reactions. This is not unexpected as generally the presence of surface oxygen is the determining factor in adsorption (Essington, 2003). It is unknown at this point whether these groups are located internal to the structure of graphite or are merely located at the edge of each plane of C=C bound atoms.

This result of a potentially mixed substance between graphite and graphite oxide is informative as XRD analysis of the experimental graphite showed a very clear graphite spectrum. Spectra of graphite oxide have been made and they

show significant differences when compared to the spectra measured of the experimental graphite. This, combined with the initial work by Friedel & Carlson, suggests that the existence of these groups is characteristic to natural graphite to a certain degree. As the presence of these groups did not result in a shift of the XRD spectra, it is believed that they represent a small fraction of the available surface. It should be noted that this could also be due to a lack of coordinated far ordering in the sample. This possibility cannot be ruled out but it is unlikely that if the graphite was significantly oxidized no far ordered graphite oxide would result. In either case, this does suggest that a measurement of this functionalization is important for an analysis of the sorbing behavior of graphite.

Additional implications to the chemistry of the adsorption reaction from the above analysis and the PZC measurement will be discussed in the following sections.

4.2 Chemistry of Adsorption

One of the primary requirements for being able to calculate stability constants for the formation of a surface-ion complex is the identification of the sorbing species and surface site. Uranium chemistry is complex in solution and the identification of a sorbing species was one of the primary goals of this research. The data suggests the existence of more than one sorbing species of interest for uranium in solution with graphite. Shown below in Figure 4.1 is an overlay of uranium speciation under experimental conditions with the mass percentage sorbed.

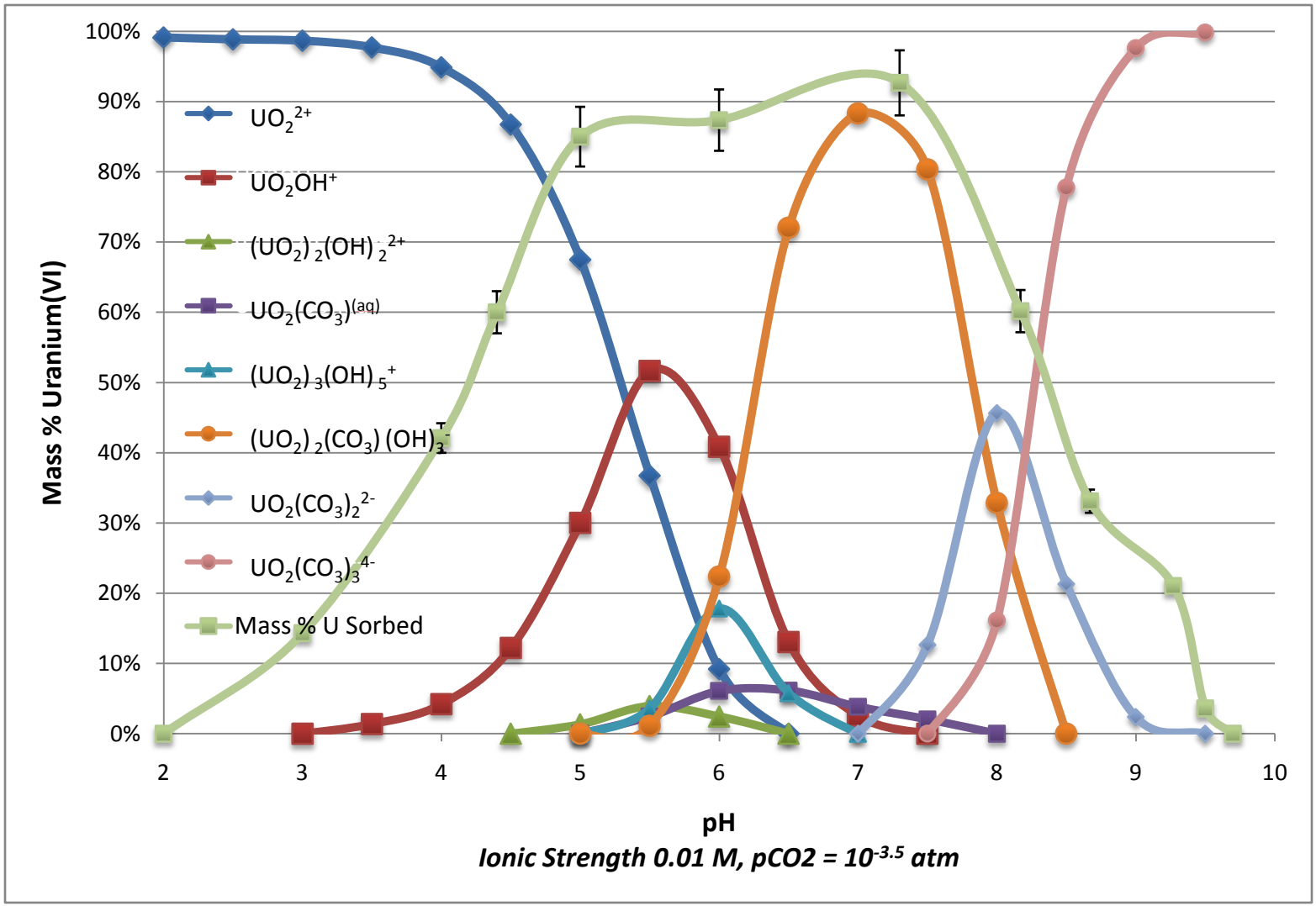

Figure 4.1: Uranium Speciation from EQ3/6 overlaid with mass percentage uranium sorbed

As can be seen in Figure 4.1 above, there is no easy map between any one uranium species in solution and sorption behavior with graphite which suggests that one solution species does not dominate the sorption behavior. It can also be noted that sorption remains at a maximum and continues to occur even when the dominant ions in solution change from positive to negative species. One hypothesis that has been proposed in the literature to explain uranium sorption to other materials is that UO_2OH^+ and $(UO_2)_2(CO_3)OH_3^-$ are the species primarily responsible for uranium sorption (Ho & Miller, 1986 and Sagert *et al*., 1989). This idea was proposed as there appears to be good experimental agreement between the relative concentrations of UO_2OH^+ and $(UO_2)_2(CO_3)OH_3^-$ and the relative mass sorption. While those species may be contributory in nature to the sorption, this research suggests that they cannot be the only species of interest in solution. Closer examination of sorption data taken at pH = 3 suggests that that hypothesis cannot explain all the experimental data produced in this work. Relevant speciation data are summarized in Table 4.4 below:

Species	Concentration (Molality)	Mass % U
UO_2^{++}	2.07×10^{-6}	98.1043%
UO_2Cl^+	1.90×10^{-8}	0.9005%
UO_2OH^+	9.14×10^{-10}	0.0433%
UO_2^+	8.02×10^{-11}	0.0038%
$(UO_2)_2OH^{+++}$	8.75×10^{-12}	0.0004%

Table 4.4: Detailed Uranium Speciation at pH = 3 under experimental conditions using EQ3/6

As can be seen in the data above for uranium speciation under the 500 ppb experimental concentration level, UO_2^{++} is the dominant solution species and UO_2OH^+ represents only 0.0433% of all uranium in solution. When this fact is considered with the fact that under these conditions 14.3% of uranium mass in solution sorbs to the graphite, it appears unlikely that the presence of this species is a determining factor. If that were the case, that such a small solution concentration could give rise to that level of sorption, when the concentration of UO_2OH^+ rises to 4.21% by mass at pH = 4 a significantly stronger increase in sorption would be expected than merely the rise from 14.3% to 42.1% of uranium in solution sorbed. It would seem strange that a 2000% increase in solution concentration of the primary sorbing species would yield a not even 300% increase in mass sorbed. This suggests that at a minimum the pure UO_2^{++} ion can form a complex with graphite as this species dominates the solution at pH = 3 and remains in solution at significant levels until pH = 6.5.

However, this cannot provide a complete understanding of the complexation on the graphite surface as strong sorption (~25% U mass in solution) can still be seen in the alkaline region (pH = 9) where UO_2^{++} has a mass concentration of 5.82×10^{-18} M (EQ3/6). At this pH, the two dominant uranium species in solution are $UO_2(CO_3)_3^{4-}$ (97.61% U by mass) and $UO_2(CO_3)_2^{2-}$ (2.37% by mass) with no other uranium species having a mass concentration greater than 0.001% (EQ3/6). This is indicative of a carbonate species participating in a surface complexation reaction with graphite which is an interesting result. Previous research has noted that uranium sorption to various media is inhibited

when uranyl carbonate species become the dominant solution species (Waite *et al.*, 1994, Hyun *et al.*, 2009, Prikryl *et al.*, 1994). This research suggests that for graphite this answer is not sufficient to explain behavior at alkaline pH. At pH = 9.27, the concentration of $UO_2(CO_3)_3^{4-}$ is 99.41% and $UO_2(CO_3)_2^{2-}$ is 0.58% of uranium in solution and mass sorption of 21.0% of uranium in solution was still observed at this point. No other uranium mass species in solution has a mass concentration greater than 0.00005%. This would seem to suggest that for graphite the presence of dissolved CO_3^{2-} is more important than the presence of uranyl carbonate species. It is interesting to note that at approximately the same pH where sorption is reduced to negligible in the alkaline region (pH=9.5), the concentration of dissolved CO_3^{2-} under atmospheric conditions is almost the exact concentration of uranium used in those experiments at 2.1×10^{-6} M. It is unknown if this is a coincidence or indicative of some other feature of the system.

At this point, it would seem reasonable to conclude that the sorbing species of interest are, at the minimum, the UO_2^{2+} ion at acidic pH and some form of complexed carbonate ion at alkaline pH. If the UO_2^{2+} ion is indeed complexing with the uranium, that would suggest that a positively charged ion is sorbing to a positively charged surface as indicated by the pH being below the PZC of 9.3. This suggests that one of the reasons why sorption begins to significantly rise after pH = 3 is that, as can be seen from Figure 3.4, the surface is becoming, while still net positively charged, more negatively charged as surface sites are deprotonated. If this is true, a surface complex would be formed between the UO_2^{2+} ion in solution and the surface at one or more deprotonated

C-OH sites and more of these sites are available as pH approaches the PZC. That fact counteracts the decrease in solution concentration of UO^{2+} that is simultaneously occurring. A prospective reaction for this complex is shown below as Equation 4.1.

$$UO_2^{2+} + \equiv C - (OH)_2 \rightarrow (\equiv C - O_2)UO_2^0 + 2H^+ \qquad Equation\ 4.1$$

A bidentate structure is proposed to achieve an overall electrical neutrality of the surface complex formed. However, this one complex is not sufficient able to explain sorption behavior over the entire experimental region.

At pH=9.27, the concentration of the free uranyl in solution is approximately 2.5 X 10^{-19} M or approximately 0.00000000012% of the total uranium mass in solution (EQ3/6) at a point where 21.0% of the mass in solution sorbs. As discussed above, a surface complex between some uranyl carbonate species and the graphite surface is proposed. Two potential reactions that would explain the data are listed as Equations 4.2 and 4.3.

$$UO_2(CO_3)_2^{2-} + \equiv C - (OH) \rightarrow \equiv C - O - UO_2(CO_3)_2^{3-} + H^+ \qquad Equation\ 4.2$$

$$UO_2(CO_3)_2^{2-} + \equiv C - (OH_2)^+ \rightarrow \equiv C - OH - UO_2(CO_3)_2^{2-} + H^+ \qquad Equation\ 4.3$$

While these complexes would be negatively charged, the available data does not have the ability to suggest anything beyond the formation of a uranyl carbonate surface complex. There are many potential complexes that could

satisfy this requirement and further investigation would have to be performed to distinguish between them.

More evidence for the existence of multiple sites is provided by Sposito (1980), in a mathematical derivation for the Freundlich adsorption isotherm as a sum of series of sorption sites that are each governed by independent Langmuir isotherm equations. A single Langmuir description of the data was rejected because of the curved residuals and several assumptions which would be mutually exclusive when applied to this data. The Langmuir model requires that all adsorption sites are identical and requires that adsorbed species do not interact. These assumptions when considered together are unable to account for the large initial sorption observed and the slower phase that then occurs and the incomplete recovery of sorbed uranium. If sites were homogenous and species were not interacting, kinetics would be expected to be identical and identical fractions of uranium would be expected to desorb regardless of initial uranium concentration in solution. Below is the Freundlich equation that was produced for the experimental work at pH = 5 (Equation 3.3).

$$q = K_F c_{eq}^N = 0.930\ c_{eq}^{0.37} \qquad Equation\ 3.3$$

In the mathematical derivation of the Freundlich isotherm by Sposito, it was shown that the value of the exponent *N* is a measure of the heterogeneity of the site surface. As *N* varies closer to 0, the number of sites that the sorbing species of interest is complexed with increases. The exponent calculated for the experimental work in this case has a value of 0.37 which indicates that surface

heterogeneity is a good assumption which fits with the experimental data. This data provides evidence for a multi-species model complex.

At this point, the exact complexation reaction that is occurring cannot be determined with precision beyond being able to state that this work suggests the sorption of the pure UO_2^{2+} ion and a uranyl carbonate species. Unfortunately, detailed knowledge of the complexation reaction is required for application of any of the surface complexation models described in Section 1 but conclusions can still be reached about the type of model that would be appropriate for this type of reaction.

4.3 Surface Complexation Models

For the three different types of surface complexation models discussed in Section 1, attempts were made to determine which model would fit the experimental data most precisely.

4.3.1 Constant Capacitance Model

It is not believed that the development of a CCM would fit the experimental results. As the CCM is unequipped to model the formation of anything beyond strong inner-sphere complexes, a CCM would have difficulty explaining the incomplete desorption and kinetics results shown in Sections 3.3 and 3.4. In the higher concentration uranium samples measured, the fact that the amount kinetically sorbed at equilibrium and available to desorb is significantly larger than the immediately sorbed, slow desorbing fraction suggests that a model that cannot consider outer-sphere weak complexes is inappropriate. Accordingly, this model was not used to evaluate the data.

4.3.2 Diffuse Layer Model

The DLM has several advantages over the CCM for modeling the interaction of uranium and graphite with the most important being the ability to consider weak electrostatically adsorbed species as well as strong inner-sphere complexes. This ability to consider both strong and weak attractions between the uranium ions and the graphite surface is believed to be vital to any model attempting to explain the experimental results. The electrostatic attraction felt be an ion in solution has been expressed as shown in Equation 4.4 (Langmuir, 1997).

$$\sigma\left(\frac{C}{m^2}\right) = 0.1174 I^{1/2} sinh\left(\frac{z\psi F}{2RT}\right) \qquad Equation\ 4.4$$

Where,
σ = Surface Charge
I = Ionic Strength of Solution
ψ = Electrical potential
z = Charge of solution electrolyte
F = Faraday Constant
R = Ideal Gas Constant
T = Temperature

This equation gives the surface charge of the adsorbing species. This surface charge is combined with a mass balance of the sorbed species to determine intrinsic complexation constants for the formed surface-ion complex. As can be noted in Equation 4.5 below, this relationship is proportional to solution ionic strength. In the experimental work described in Section 3.2, there was found to be no influence on uranium sorption by varying ionic strength under below neutral conditions. This indicates that the application of a DLM to explain uranium sorption to graphite is inappropriate.

4.3.3 Modified Triple Layer Model

The modified TLM describes the surface charge by Equation 4.5 below (Essington, 2003).

$$\sigma_{is} + \sigma_H + \sigma_{os} = -\sigma_d \qquad Equation\ 4.5$$

Where,
σ_{is} = Surface charge contributed from inner-sphere complexes
σ_H= Surface charge from adsorbed hydrogen ions
σ_{os} = Surface charge from outer-sphere cation-anion complexation
σ_d = Charge density of counter-ions

This equation is solved simultaneously along with mass balance equations for the surface sites and mass balances for each different contributor to charge. The σ_d term above can be determined by the capacitance differences between the three layers of charge surrounding the surface. This yields a charge density that can be represented by Figure 4.2 below.

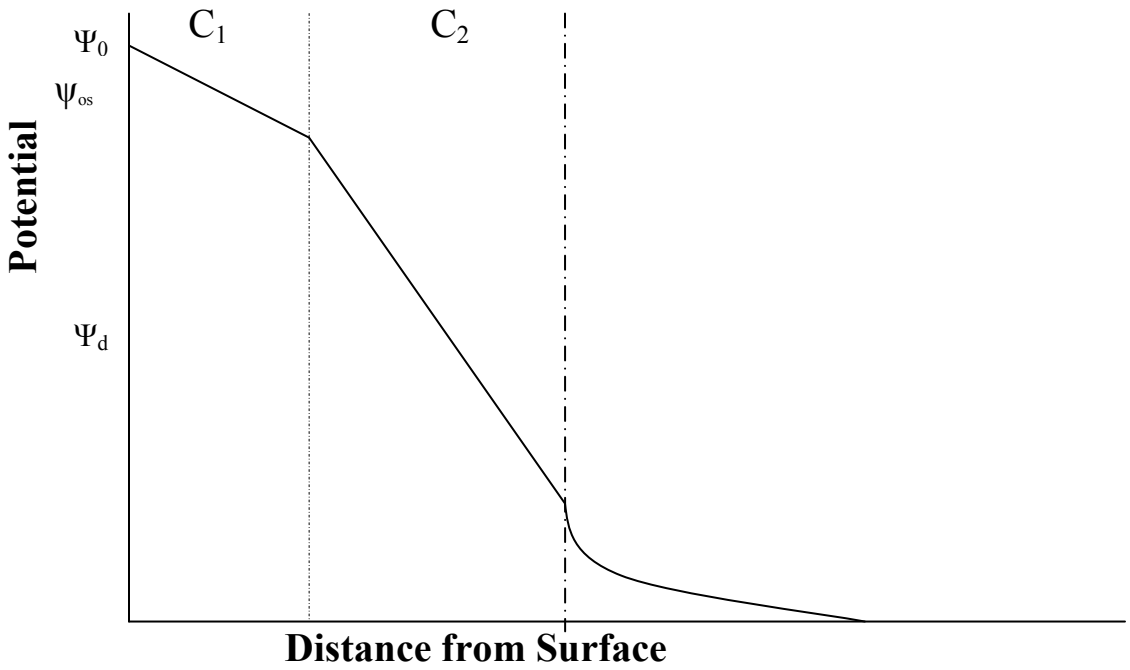

Figure 4.2: Schematic of system charge variance from surface (Adapted from Langmuir, 1997)

Where,

Ψ_0 *= Potential at surface*
Ψ_{os} *= Potential at outer sphere*
Ψ_d *= Potential at counter ion layer*
C_1 *= Integral capacitance of inner-sphere layer*
C_2 *= Integral capacitance of outer-sphere layer*

By altering the intrinsic capacitance of the inner-sphere and outer-sphere layer, this can be fit to experimental data. While it is the most complex of the three models explicitly considered in this work, it appears to have the required level of complexity to represent the uranium-graphite system. Additionally, it would be possible, based on experimental work and solution potential measurements, to explicitly calculate the complexation constants. A sample for the complexation reaction listed in Equation 4.1 is shown below as Equation 4.6 (representing the surface sites as initially unprotonated).

$$K_{UO_2^{2+}}^{int} = \frac{[(\equiv C - O_2)UO_2^0]}{[\equiv C - O_2^{2-}][UO_2^{2+}]} \exp\left(\frac{F(\psi_{is} - \psi_0)}{RT}\right) \qquad Equation\ 4.6$$

Where,

Terms are as defined above in Equation 4.4

A complete calculation of these stability constants would involve the simultaneous solving of multiple differential equations and is beyond the scope of this work. However, it is sufficient to say that a TLM would be proper for modeling the interaction of uranium and graphite.

4.4 Transport Model

At the beginning of this work, it was stated that in order to understand the reactive transport of uranium through a graphite matrix an understanding of partitioning and kinetics would have to be obtained. The above described work has provided the data necessary to model the uranium-graphite interaction and now the only question is that if that is sufficient to allow a predictive model to be developed that would be able to establish under what conditions the impact of reactive transport in a TRISO fuel element would be important.

The first thing that must be noticed is that a simple calculation of the R factor based on the equilibrium K_d values measured would be inappropriate. As shown in Section 3.3, there is a kinetic factor in the sorption of uranium to graphite. In those results, there is a fraction of uranium in solution that sorbs immediately to the graphite and then a fraction that sorbs in a manner such that kinetics cannot be discounted. When this is combined with the fast flow column experiments, also shown in Section 3.3, it is manifestly obvious that the

application of a retardation coefficient calculated from an equilibrium K_d would be highly inappropriate to modeling uranium transport through graphite.

Next attention must be drawn to the incomplete recovery in the fast flow column experiments and the incomplete desorption measured in the batch desorption experiments. During the batch desorption each sample container had approximately 0.8 g of graphite and each (excluding the 500 ppb concentration) failed to desorb approximately the same amount of uranium. This seems to suggest that a given mass of the experimental graphite has an ability to attach in a strong inner-sphere complex a set mass of uranium without regard to total solution concentration. Beyond this mass amount, a linear relationship between solution concentration and K_d can be derived for uranium concentrations sufficient to exceed the amount that can be complexed by the fast sorbing fraction. It can also be seen that below this mass amount in solution, a linear relationship between solution concentration and K_d can be derived as well. This is shown graphically for the pH 5 isotherm below in Figure 4.3.

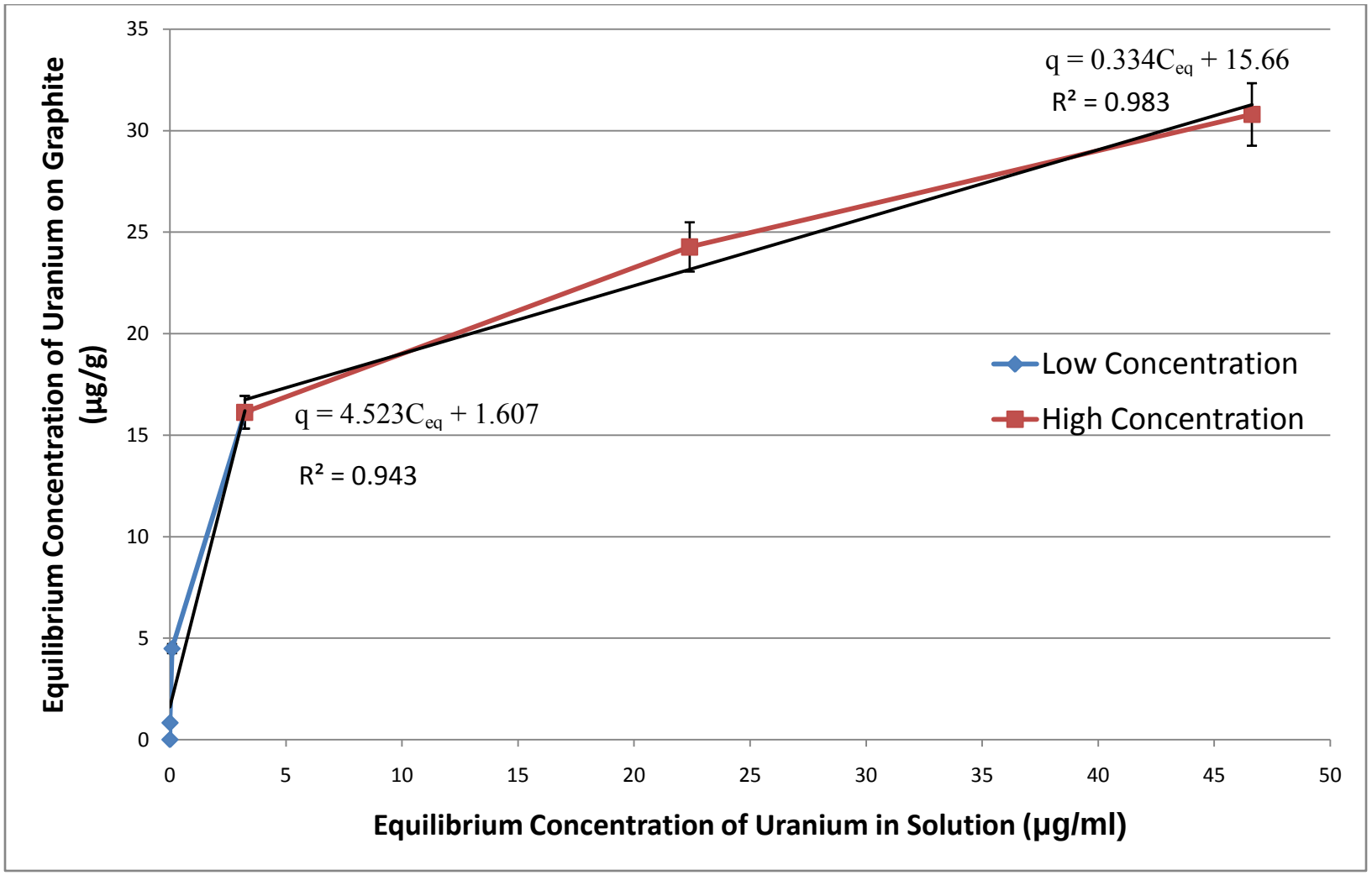

Figure 4.3: Linear Isotherm Fitting for pH = 5 data

Figure 4.3 indicates that for modeling purposes a double linear model would be an appropriate assumption to make to use this data. The very high values for R^2 (0.943 and 0.983, for low and high concentration regions respectively) suggest that each linearization is successful at explaining sample variation in that region. The information contained in the figure can be used to calculate the required number and value of partition coefficients needed for modeling purposes. In this case, equilibrium concentrations of uranium greater than 3.23 ppm would require the use of both equations. It should be noted at this point that no conclusions are made about partitioning and retardation at mass concentrations in the concentration region beyond the batch experiments performed for this work and further investigation would have to be performed to integrate that information into this model. Similarly it must be noted that the linear equations above were calculated using the measured equilibrium concentrations of uranium in solution and on the graphite which is information that is unlikely to be available. However, information about the initial concentration of uranium in solution can be obtained by using the degradation information of the TRISO particles given in Section 1 and by making assumptions about the behavior of the TRISO particles in a repository environment. This would permit the calculation of different source terms for uranium release which would permit calculation of initial mass concentrations in solution. This calculated initial concentration would always be above the equilibrium concentration of uranium which means that it could still be used in the linear equations above as a conservative assumption.

However, as was noted in Section 3.3, there is non-linear kinetic component of uranium sorption to graphite that cannot be ignored in modeling reactive transport of uranium through a graphite matrix since the actual water velocity through a TRISO fuel compact after irradiation is presently unknown. As a point of comparison, shown below in Table 4.5 are typical values for pore velocity for various geological media as well as the time water moving at that speed would require to move half the length (0.395 m) of a TRISO fuel compact.

Material	Groundwater Velocity (m/s)	Travel Time (hrs)
Sand	$10^{-2} – 10^{-6}$	0.01 – 109
Basalt	$10^{-2} – 10^{-7}$	0.01 – 1010
Silty Sands	$10^{-5} – 10^{-7}$	11 – 1010
Glacial Till	$10^{-6} – 10^{-12}$	$1.01 X10^{4} – 1.01 X10^{8}$
Shale	$10^{-9} – 10^{-13}$	$1.01 X 10^{5} – 1.01 X 10^{9}$
Dense Igneous Rock	$10^{-10} – 10^{-14}$	$1.01 X 10^{6} – 1.01 X 10^{10}$

Table 4.5: Typical groundwater velocities (From Langmuir, 1997) and calculated time to move 395 mm

As the long kinetic component is on the order of hours, it can be noted that, depending on flow characteristics through the TRISO element, the kinetic component could either be of significance or not. In this work, kinetics had to be considered due to the experimental conditions. The non-linearity in the kinetic response was dealt with by partitioning the response into an equilibrium fraction and a kinetic fraction.

The value of any theory is in its ability to provide verifiable hypotheses about physical events. In this case, now that an understanding of the uranium/graphite sorption system has been experimentally reached, the question must be: Can an accurate prediction of uranium transport behavior through a graphite matrix be made? The theoretical understanding was tested by inputting theoretical and experimentally generated parameters into CXTFIT to generate a theoretical model. A solution concentration of 10 ppm was selected as no experimental data had been taken at that specific point and the mass concentration appears to be above the limits of the equilibrium fraction as discussed below. The general details of the model used are as follows:

- Transport behavior has an equilibrium fraction and a kinetic fraction
- The equilibrium fraction has a significantly higher partition coefficient than the kinetic fraction and the K_d is modeled by the low mass relationship between solution/solid concentration shown above
- The equilibrium fraction must be completely filled before the kinetic fraction becomes involved in partitioning.
- The kinetic fraction was modeled by using a first-order rate constant equivalent to $\alpha = 0.01925\ hr^{-1}$ (Calculated from high mass partitioning half-time of 36 hours)
- The kinetic fraction has a lower partition coefficient that can be modeled by the high mass relationship between solution/solid concentration shown above.

- The equilibrium fraction maximum loading for the experimental graphite used corresponds to 1.7 μg U / g graphite (From kinetics results).

The 10 ppm solution was then flowed through a Flex Column from KONTES as described in Section 2.6. The specific details of the column are shown in Table 4.6 below.

Dispersion Coefficient	0.903 cm^2/hr
Column Area	0.3845 cm^2
Elution Rate	0.25 cm^3 / min
Column Length	9 cm
Graphite Mass	2.27 g
Graphite Bulk Density	1.794 g/cm^3
Porosity	0.365

Table 4.6: Experimental conditions for model validation

A picture of the experimental set-up is shown as Figure 4.4 below. A graph of the model predictions is shown after as Figure 4.5 (Note: CXTFIT results for uranium are sum of two computational calculations due to program restrictions).

Figure 4.4: Model Validation Experiment

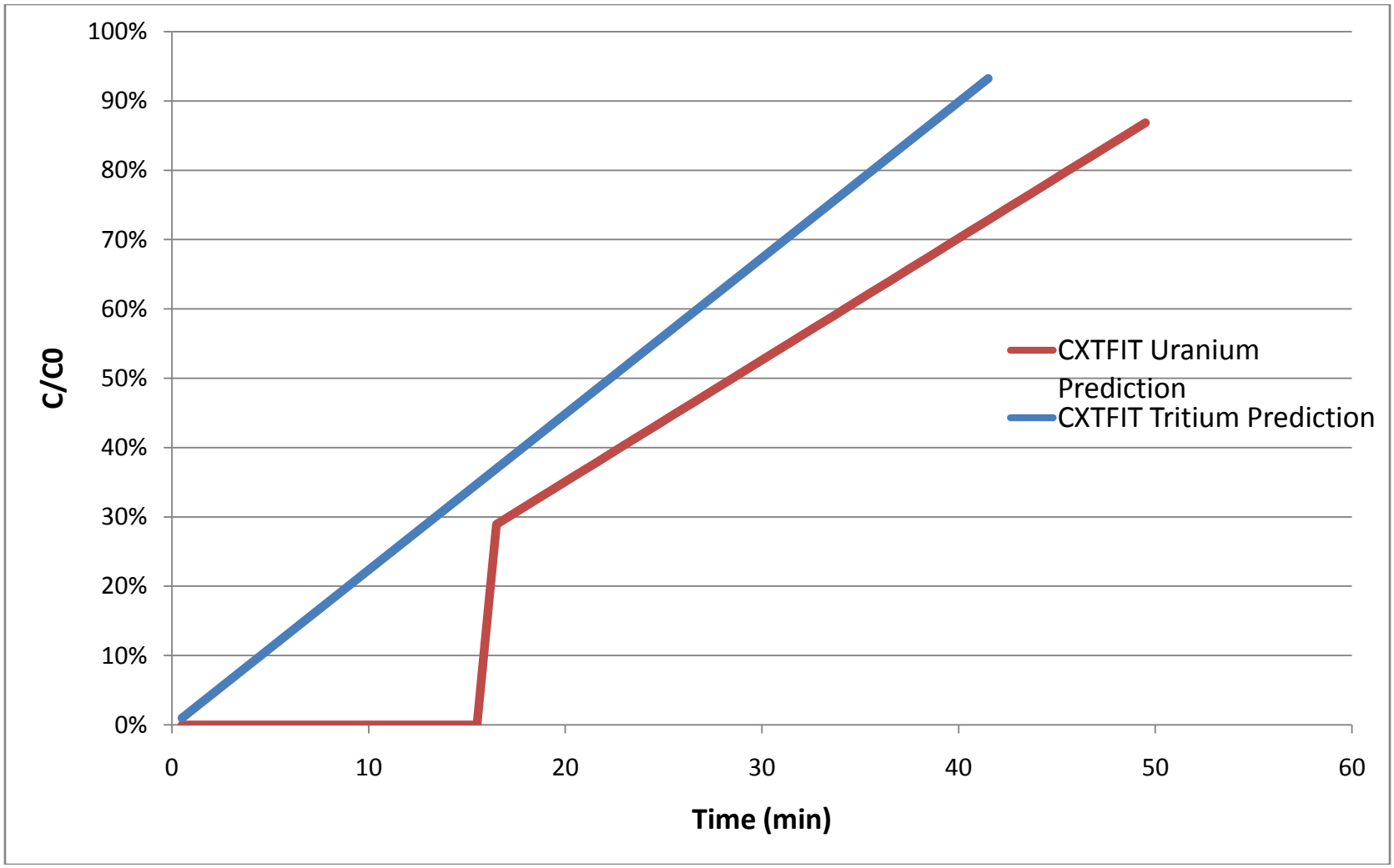

Figure 4.5: CXTFIT Predicted Response using the reactive transport model developed

The CXTFIT results reflect the fact that a fraction of the uranium immediately partitions to the graphite surface. This fraction, according to the retardation factor calculated, will be delayed beyond the time scale of the experiment. It should be noted at this point that the interactions between low concentration uranium solutions and graphite have been modeled as an equilibrium process on the basis of the fast kinetics in this region. It is possible that this is an inaccurate assumption with evidence being the incomplete recovery of uranium during desorption experiments. This is evidence, at minimum, of hysteresis in the forward and backward partitioning reactions between uranium and graphite in solution and potential evidence of irreversibility in the uranium/graphite partitioning reaction. In this case, it appears that the backward reaction is significantly slower than the forward reaction (which is effectively immediate). However, the time scale that would be required to investigate the influence of this hysteresis renders it experimentally unfeasible for this work. For the validation study performed, it is irrelevant as the time scale is insufficient to see an increase in eluted uranium concentration that could be attributed to the breakthrough of the retarded low-mass fraction. In any case, the assumption of equilibrium instead of hysteresis or irreversibility provides additional conservatism to the model.

Additionally, it should be noted that the shape of both the predicted uranium and tritium breakthrough curves do not follow a traditional sigmoid curve that would be expected for breakthrough of either a reactive or non-reactive tracer. The shape does in fact more closely resemble a limiting systematic case

where mechanical dispersion is of much higher significance than fluid flow velocity. This can be explained as the dispersion coefficient used in the model implementation was obtained through a separate experiment where tritium alone was run through a column and the effective dispersion coefficient was calculated from that using CXTFIT and the measured breakthrough curve. This effective dispersion coefficient also includes non-ideal deviations from the perfectly ideal case of a parabolic flow profile within it. In this case, it seems likely that the existence of a boundary layer of significant thickness, relative to the area of flow, has resulted in an apparent dispersion that is larger than what should be expected leading to the non-traditional breakthrough shape. In this case, an estimate of the non-ideality can be obtained by using Equation 4.7 to generate a theoretical estimated dispersion coefficient and comparing that to the experimentally calculated coefficient.

$$D = \alpha \cdot v \qquad Equation\ 4.7$$

Where,
D = Mechanical Dispersion Coefficient, cm^2/hr
α = Dispersivity, can be approximated by median particle diameter, cm
v = Water velocity, cm/hr

Using the known qualities of the graphite and the column with Equation 4.7, an estimate of the mechanical dispersion is 0.59 cm^2/hr for the column system. It can thus be seen that the dispersion coefficient used is roughly half again higher than would be expected indicating that significant non-ideal factors are included in the effective dispersion coefficient. However, as these non-idealities will affect both tritium transport and uranium transport equally, the

CXTFIT calculations remain a valid way of comparing model predictions to empirical data.

For a 10 ppm U solution, the calculated retardation of the low mass equilibrium fraction is a factor of 25.65 (corresponding to a K_d of 5.02 ml/g). The calculated maximum retardation factor for the high mass kinetic fraction is 10.33 (corresponding to a K_d of 1.9 ml/g). Accounting for travel time through the graphite with the kinetic factor, the effective retardation factor that should be observed during the validation study should be 1.11. As the study performed will not be sufficiently long to see the elution of the retarded kinetic fraction, the apparent retardation provides a method of quantifying the accuracy of the estimates of α and R. Figure 4.6 below shows the actual breakthrough curves measured during the study with the CXTFIT predicted curves.

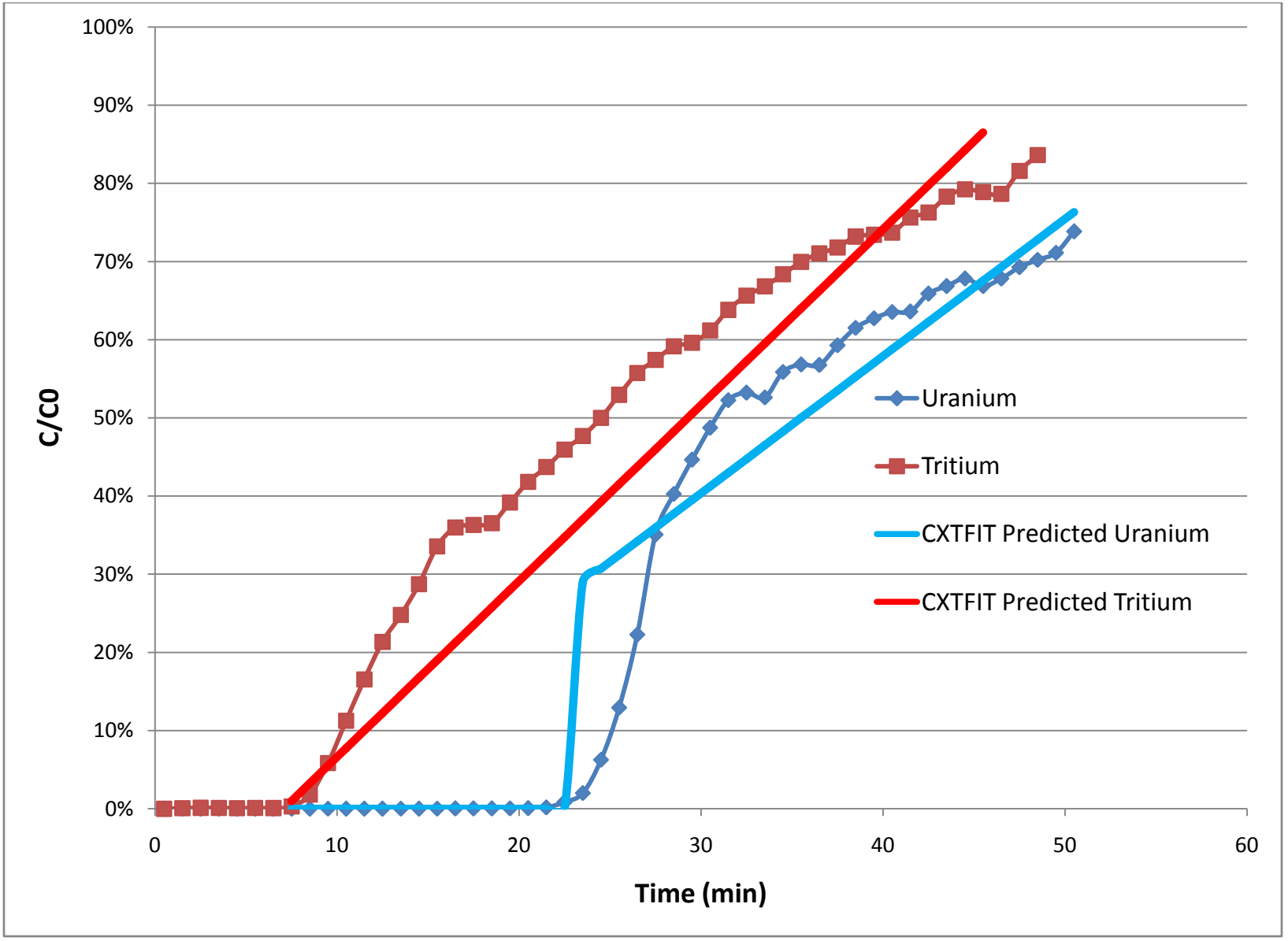

Figure 4.6: Comparison of CXTFIT Predicted Results with Actual Results Uranium and Tritium Breakthrough

As can be seen above there is good general agreement between the predicted breakthrough curves and the actual breakthrough curves. As the predicted breakthrough curves were generated at a point that lacked experimental data, this provides evidence that the model can be generalized to the experimental mass region (0.5 – 50 ppm). The effective retardation factor can be estimated as a first approximation from the ratio of the experimental slopes as shown below in Equation 4.7.

$$R = \frac{Velocity_{Tritium}}{Velocity_{Uranium}} = \frac{Slope_{Tritium}}{Slope_{Uranium}} = \frac{1.045}{0.891} = 1.17 \qquad Equation\ 4.7$$

As the predicted effective retardation factor was 1.11, the error can be estimated as $\left(1 - \frac{(1.11-1)}{(1.17-1)}\right) = 0.35$. This indicates that the model over-predicted the release of uranium by 35% for the kinetic fraction. Additionally, the model underestimated the amount of uranium that would partition to the highly retarding high-mass site. This was quantified by comparing the predicted fast fraction retained mass to the actual fast fraction mass retained $\left(\frac{Actual\ Mass\ Retained\ \mu g}{Predicted\ Mass\ Retained\ \mu g} - 1 = \frac{(3.82+2.11)}{(3.82)} - 1 = 0.55\right)$. This indicates that 55% more uranium was retained in the fast fraction than was predicted by the model in this case. This means that for both the equilibrium fraction and the kinetic fraction the model was accurate to within an order of magnitude of experimental results. The fact that for both fractions the model underestimated release can most likely be attributed to the conservative assumptions that were incorporated into the

model's structure. However, this is not necessarily a negative from a safety point of view.

This shows that the model has good agreement with experimental data for a point at which experimental data was not used in the creation of the model. The basic assumptions that were used could be adapted to different environments and by varying values of α, [U] and the fraction of kinetic and immediate sorbing sites, this model could then be adapted to provide an estimate of the necessity of incorporating reactive transport in a TRISO fuel element into repository performance.

CHAPTER 5

CONCLUSIONS AND FUTURE WORK

If HTR reactors are to see wide spread adoption, decisions will have to be made about the final disposition of TRISO fuel and if an informed decision is to be made, the potential consequences of each decision must be examined. The options for disposal must include the most obvious option which is direct disposal of the spent TRISO fuel element in a geologic repository. To properly evaluate the consequences of this decision, the large mass of graphite in a TRISO fuel element would have to be incorporated into a repository performance assessment.

This research has shown that the uranium/graphite system is complex due to the innate complexity of both uranium solution chemistry and the complexity and variability in the composition of graphite. Nevertheless, several important conclusions about the potential repository performance of TRISO fuel can be drawn from the experimental work in this research as well as in the model developed. The first is that to explain uranium transport through graphite by means of a single K_d and its associated retardation factor would be inappropriate due to a measured kinetic response and non-linearity in partitioning with mass. Second, graphite has shown the ability to strongly complex and significantly retard uranium in solution under environmentally relevant conditions ($5 < pH < 8$, $[CO_2] = 350$ ppm) up to a mass concentration of 50 ppm with some evidence existing of irreversibility of this complexation. Third, this partitioning is insensitive to ionic strength below neutral pH but is sensitive to pH and to the concentration

of dissolved carbonate. Fourth and finally, while neglecting uranium retardation by graphite would always be a conservative assumption, it could in some instances significantly underestimate the repository performance of TRISO fuel. This could be important in the near time frame on geological time scales as the TRISO particles themselves fail and release low concentrations of uranium that this work indicates would be strongly complexed by the graphite matrix.

While this work provides for several conclusions relevant to the chemistry of the graphite/uranium interaction and the effect on repository performance by incorporating the graphite surrounding directly disposed of TRISO fuel, it has also suggested several areas where additional knowledge would be desirable. Accordingly, a proposal for future work would include the following items:

- Experiments with different graphite and graphite oxide to attempt to understand what role graphite oxide functional groups play in uranium sorption
- Investigation into whether incomplete desorption suggests actual irreversibility or hysteresis
- Investigation of graphite with complexed uranium by Extended X-Ray Absorption Fine Structure (EXAFS) or some other technique that would allow the direct analysis of the formed uranium-graphite complexes
- Completion of a Triple Layer Model to estimate stability constants for uranium/graphite complexes
- Expand partitioning research to other radionuclides of interest such as Np-237, Pu-239, Tc-99 and others

- Examination of nuclear graphite by the same physical and electronic methods performed here to permit the adaptation of the model for reactive transport proposed here to nuclear graphite
- Combining the transport model developed here with a source term developed from the corrosion and flawed manufacture of TRISO particles to permit actual performance estimates for the fuel

This work has provided data on what parameters partitioning in the uranium/graphite system is sensitive too. It has shown that even under fast flow conditions retardation of uranium can be significant to a mass level that is over 30 times the current EPA drinking water standard and that for common groundwater flow speeds, retardation of uranium in graphite can be significant to several orders of magnitude beyond that. This work indicates that under a wide variety of conditions, studies should be done to quantify the delay in release from any repository accepting large quantities of TRISO fuel due to the presence of graphite and this work also indicates the relative importance of various systematic conditions.

REFERENCES

Ackay, H. (1998) “Aqueous speciation and pH effect on the sorption behavior of uranium by montmorillonite.” Journal of Radioanalytical and Nuclear Chemistry, **237**(1-2) 133-137

Baik, M. H., S. P. Hyun, P. S. Hahn, (2003) “Surface and Bulk Sorption of Uranium(VI) onto Granite Rock” Journal of Radioanalytical and Nuclear Chemistry **256**(1) 11-18

Bodansky, D. (2004) Nuclear Energy: Principles, Practices and Prospects, Springer Publishing, ISBN: 978-0387207780

Brunauer, S. E., P. H.; Teller, E. (1938). "Adsorption of gases in multimolecular layers." J. Am. Chem. Soc., vol. 60, p. 309-319 (1938). **60**: 309-319

Bissessur, R. *et al*. (2006), “Intercalation of Polypyrrole into Graphite Oxide,” Synthetic Materials, **156** pp. 1023-1027

Davis, J.A. & D.B. Kent, (1990), “Surface Complexation Models in Aqueous Geochemistry,” Mineral-Water Interface Chemistry, Mineral Society of America pp. 177-260.

Davis, J. A., D. E. Meece, *et al*. (2004). “Approaches to surface complexation modeling of Uranium(VI) adsorption on aquifer sediments.” Geochimica et Cosmochimica Acta, **68**(19) 3621-3641

Echevarria, G., M. I. Sheppard, *et al*. (2001). "Effect of pH on the sorption of uranium in soils." Journal of Environmental Radioactivity **53**(2): 257.

Essington, M. E. (2003), Soil and Water Chemistry: An Integrative Approach, CRC Press, ISBN: 978-0849312588

Fachinger, J. A., M den Exter, *et al*. (2006) “Behaviour of spent HTR fuel elements in aquatic phases of repository host rock formations” Nuclear Engineering and Design, **236** 543-554

Fachinger, J. A., W. von Lensa, T. Podruhzina, (2008). “Decontamination of nuclear graphite” Nuclear Engineering and Design, **238** 3086-3091

Francis, A. J. (1998). "Biotransformation of uranium and other actinides in radioactive wastes." Journal of Alloys and Compounds **271-273**(0): 78-84.

Friedel, R.A. and G.L. Carlson (1971), “Infrared Spectra of Ground Graphite,” Journal of Physical Chemistry, 75(8)

General Atomics, (1996) “Gas Turbine-Modular Helium Reactor (GT-MHR) Conceptual Design Description Report.” **GA Project No. 7658**, San Diego, CA

Golub, D., A. Soffer, Y. Oren (1989), “The Electrical Double Layer of Carbon and Graphite Electrodes Part V. Interactions with Simple Ions,” Journal of Electroanalytical Chemistry **260** pp 383-392

Gray, W. J., (1982), “A Study of the Oxidation of Graphite in Liquid Water for Radioactive Waste Storage Applications.” Proc. Radioactive Waste Manage. **3**(2) 137-149

Ho C.H. & N.H. Miller, (1986), “Adsorption of Uranyl Species from Bicarbonate Solution onto Hematite Particles,” Journal of Colloid Interface Science, **110**, 165-171

Hyun, S. P., P. M. Fox, *et al*. (2009), “Surface Complexation Modeling of U(VI) Adsorption by Aquifer Sediments from a Former Mill Tailings Site at Rifle, Colorado” Environ. Sci. Technol. **43**(42) 9368–9373

Janowska, I. *et al.*, (2010), “Microwave Synthesis of Large Few-Layer Graphene Sheets in Aqueous Solution of Ammonia,” Nano Research, **3**(2) pp. 126-137

Kandah, I.S., *et al.*, (2006), “Synthesis and Characterization of Activated Carbon From Asphalt,” Applied Surface Science 253 pp. 821-826

Kaplan, D.I., T. L. Gervais, *et al.* (1998), “Uranium(VI) sorption to sediments under High pH and Ionic Strength Conditions,” Radiochimica Acta **80**(4)

Kercher, A. K., J. D. Hunn, *et al.* (2008), “Automated Optical Microscopy of Coated Particle Fuel.” Journal of Nuclear Materials, **380** 76-84

Langmuir, D. (1997) Aqeuous Environmental Geochemistry, Prentice Hall, ISBN: 978-0023674129

Lifang, T, M. Wen, *et al*. (2009), “Disintegration of graphite matrix from the simulative high temperature gas-cooled reactor fuel element by electrochemical method.”, Electrochimica Acta **54** 7313-7317

Mermoux, M., Y. Chabre, *et al.*, (1991), “FTIR and ^{13}C NMR Study of Graphite Oxide,” Carbon, **29**(3) pp. 469-474

Morris, E. E., T. H. Bauer (2005), “Modeling of the Repository Behavior of TRISO Fuel.” Nuclear Engineering Division, Argonne National Laboratory

Murphy, R. J., J. J. Lenhart, B. D. Honeyman, (1999), “The sorption of thorium (IV) and uranium (VI) to hematite in the presence of natural organic matter.” Colloids and Surfaces A: Physiochemical and Engineering Aspects **157** 47-62

Nickel, H., H. Nabielek, (2002) “Long-term Experience with the Development of HTR Fuel Elements in Germany.” Nuclear Engineering and Design, **217** 141-151

Petti, D. A., J. Buongiorno, *et al.* (2003) “Key differences in the Fabrication, Irradiation and High Temperature Accident Testing of US and German TRISO-coated Particle Fuel, and Their Implications on Fuel Performance.” Nuclear Engineering and Design **222** 281-297

Prikryl, J. D., A. Jain, *et al.* (2001). "Uranium(VI) sorption behavior on silicate mineral mixtures.” Journal of Contaminant Hydrology **47** 241-253

Prikryl, J. D., R. T. Pabalan, *et al.* (1994). "Uranium sorption on alpha-alumina: Effects of pH and surface-area solution-volume ratio." Radiochimica Acta **66- 7**: 291.

Prikryl, J. D & R. T. Pabalan (1999). "Sorption of Uranium(VI) and Neptunium(V) by Surfactant-Modified Natural Zeolites." Scientific Basis for Nuclear Waste Management XII pp.1035

Rangel-Mendez, J.R. & M. Streat (2002), “Adsorption of Cadmium by Activated Carbon Cloth: Influence of Surface Oxidation and Solution pH,” Water Research 36 pp. 1244-1252

Sagert, N.H., *et al*., (1989), “The Adsorption of Uranium(VI) onto a Magnetite solution,” Journal Colloid Interface Science, **130** pp. 237-247

Simunek, J., M. Th. Van Genuchten, M. Sejna, N. Toride and F.J. Leij (1999), “The STANMOD Computer Software for Evaluating Solute Transport in Porous Media Using Analytical Solutions of Convection-Dispersion Equation,” International Ground Water Modeling Center, Colorado School of Mines, Available from US Department of Agriculture

Sposito, G. (1980), “Derivation of the Freundlich Equation for Ion Exchange Reactions in Soils,” Soil Sciences Society of America Journal, **44** pp.652

Stuart, B. H. (2004), Infrared Spectroscopy: Fundamentals and Applications, Wiley ISBN: 978-0470854280

Sunwoo, S., J.H. Kim *et al.* (2000) “Preparation of ZrO_2 Coated Graphite Powders,” Journal of Materials Science **35** pp. 3677-3680

Waite, T. D., J. A. Davis, *et al*. (1994). "Uranium(VI) Adsorption To Ferrihydrite - Application Of A Surface Complexation Model." Geochimica et Cosmochimica Acta **58**(24): 5465.

Wolery, T.J. & S. A. Daveler (1993), “EQ3/6 Software Package: User’s Guide and Related Documentation,” Version 7, Available from Lawrence Livermore National Laboratory

VITA

Graduate College
University of Nevada, Las Vegas

Gregory Schmidt

Degree:

Bachelor of Science, Biological and Environmental Engineering, 2008
Cornell University

Thesis Title: Analyzing the Impact of Reactive Transport on the Repository Performance of TRISO Fuel

Thesis Examination Committee:

Chairperson, Dr. William Culbreth, Ph.D.
Committee Member, Dr. Ralf Sudowe, Ph.D.
Committee Member, Dr. Yitung Chen, Ph.D.
Committee Member, Dr. Robert Boehm, Ph.D.
Graduate Faculty Representative, Dr. Gary Cerefice, Ph.D.